© 2018. Published by The Company of Biologists Ltd | Journal of Cell Science (2018) 131, jcs213447. doi:10.1242/jcs.213447

CORRECTION

Leucine-rich repeat-containing 8B protein is associated with the endoplasmic reticulum Ca^{2+} leak in HEK293 cells (doi: 10.1242/jcs.203646)

Arijita Ghosh, Nitin Khandelwal, Arvind Kumar and Amal Kanti Bera

There were errors published in *J. Cell Sci.* (2017) **130**, 3818-3828 (doi: 10.1242/jcs.203646).

The incorrect actin loading controls were used for Fig. 1A and Fig. 3C. The corrected figure panels are shown below.

The authors apologise to readers for any inconvenience caused.

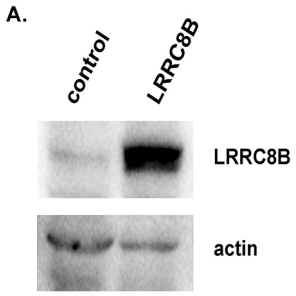

Fig. 1. Overexpression of LRRC8B attenuates the ATP-induced $[Ca^{2+}]_c$ rise. (A) Western blot showing the overexpression of LRRC8B in HEK293 cells following transient transfection. β-actin was used as a loading control.

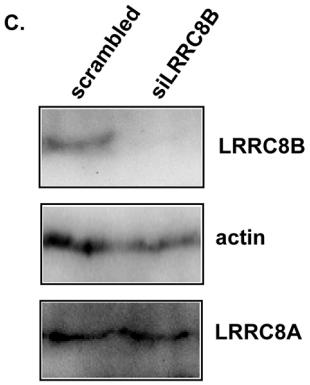

Fig. 3. LRRC8B regulates the ER Ca^{2+} pool. (C) Western blot showing the siRNA (50 nM)-mediated knockdown of endogenous LRRC8B expression in HEK293 cells. β-actin was used as an internal control. The expression level of LRRC8A was not affected.

© 2017. Published by The Company of Biologists Ltd | Journal of Cell Science (2017) 130, 3818-3828 doi:10.1242/jcs.203646

RESEARCH ARTICLE

Leucine-rich repeat-containing 8B protein is associated with the endoplasmic reticulum Ca^{2+} leak in HEK293 cells

Arijita Ghosh[1], Nitin Khandelwal[2], Arvind Kumar[2] and Amal Kanti Bera[1,*]

ABSTRACT

Leucine-rich repeat-containing 8 (LRRC8) proteins have been proposed to evolutionarily originate from the combination of the channel protein pannexin, and a leucine-rich repeat (LRR) domain. Five paralogs of LRRC8, namely LRRC8A, LRRC8B, LRRC8C, LRRC8D and LRRC8E have been reported. LRRC8A has been shown to be instrumental in cell swelling. Here, we identify LRRC8B as a key player in the cellular Ca^{2+} signaling network. Overexpression of human LRRC8B in HEK293 cells reduced the Ca^{2+} level in the endoplasmic reticulum (ER). LRRC8B-overexpressing cells exhibited a lesser release of Ca^{2+} from the ER in response to ATP, carbachol and intracellular administration of inositol (1,4,5)-trisphosphate (IP_3). LRRC8B-knockdown cells showed a slower depletion of the ER Ca^{2+} stores when sarco-endoplasmic reticulum Ca^{2+}-ATPase was blocked with thapsigargin (TG), while overexpression of LRRC8B had the opposite effect. LRRC8B-overexpressing cells exhibited a higher level of store-operated Ca^{2+} entry following store-depletion by TG. Collectively, LRRC8B participates in intracellular Ca^{2+} homeostasis by acting as a leak channel in the ER. This study gives a fundamental understanding of the role of a novel protein in the elemental cellular process of ER Ca^{2+} leak and expands the known roles for LRRC8 proteins.

This article has an associated First Person interview with the first author of the paper.

KEY WORDS: Ca^{2+} signaling, LRRC8, Pannexin, VRAC, Ion channel

INTRODUCTION

The importance of leucine-rich repeat-containing 8 (LRRC8) proteins was first realized in B cell development. Identified in a patient suffering from agammaglobulinemia, the very first reports on an LRRC8 gene highlighted the role of these proteins in B cell maturation (Kubota et al., 2004; Sawada et al., 2003). LRRC8 proteins have been so far reported in various chordates, usually as five paralogs named LRRC8A (also known as SWELL1), LRRC8B, LRRC8C, LRRC8D and LRRC8E. Bioinformatic studies have shown that LRRC8 proteins have striking similarities to the channel-forming pannexin proteins (Abascal and Zardoya, 2012). LRRC8 proteins have been predicted to evolutionarily originate from a combination of transmembrane domains of pannexin at the N-terminal and a C-terminal leucine-rich tail. Based on sequence and structural similarities with pannexins, LRRC8 proteins have also been proposed to participate in cell communication (Abascal and Zardoya, 2012). Of late, noteworthy studies from two independent groups identified LRRC8A as a component of the volume-regulated anion channel (VRAC) (Qiu et al., 2014; Voss et al., 2014).

Regulation of volume is an inherent cellular property that is executed by manipulating the passage of water and solutes across the plasma membrane. An increase in the cell volume as a result of osmotic swelling leads to an efflux of osmolytes, activating regulatory volume decrease (RVD). A multitude of channels have been proposed to contribute to swelling-induced volume perturbations (Hoffmann et al., 2009; Wehner et al., 2003). Although the existence of VRAC had been delineated earlier, the molecular entities comprising VRAC had not been identified until recently (Jentsch et al., 2016; Okada, 1997; Strange et al., 1996). With evidence favoring LRRC8A as a major VRAC candidate, a new avenue has opened up for further information on the detailed functioning of VRAC in general as well as in pathophysiology. LRRC8A was found to be indispensable for VRAC, as its knockdown suppressed endogenous outward-rectifying VRAC currents (Voss et al., 2014). A T44C mutation in the first transmembrane domain of LRRC8A rendered VRAC susceptible to modification by the sulfhydral agent 2-sulfonatoethyl methanethiosulfonate (MTSES) and resulted in altered ion selectivity, suggesting the possibility of LRRC8A being the pore-forming unit in a functional VRAC (Qiu et al., 2014). Interestingly, another study by Ullrich et al. demonstrated a role for the first extracellular loop joining the first and second transmembrane domains of LRRC8 in channel activation and ion selectivity (Ullrich et al., 2016). So far, studies on LRRC8 suggest that LRRC8A forms an essential component of VRAC in the form of a multimeric channel complex in association with other LRRC8 members, particularly LRRC8C and LRRC8D (Voss et al., 2014). Previous studies on LRRC8C and LRRC8D have revealed their participation in adipocyte differentiation and transport of small molecules, respectively (Lee et al., 2014; Tominaga et al., 2004). Recently, Syeda et al. showed that LRRC8A, along with other LRRC8 subunits formed anion selective channels when reconstituted in a synthetic lipid bilayer. The reconstituted channel was activated by osmotic gradient (Syeda et al., 2016). In rat astrocytes, LRRC8A has been shown to play a vital role in excitatory amino acid release contributing to RVD, in accordance with the role of VRAC in the process (Hyzinski-García et al., 2014). LRRC8 proteins have also been implicated in cellular uptake of platinum-class anti-cancer drugs. Cancer cells devoid of LRRC8A and LRRC8D have been shown to be resistant to cisplatin and carboplatin (Planells-Cases et al., 2015). Cisplatin has also been shown to activate LRRC8-mediated currents in *Xenopus* oocytes highlighting the role of these proteins in drug transport (Gradogna et al., 2017). Very recently, the role of VRAC has been outlined in the transport of neuroactive substances, with emphasis on LRRC8D and LRRC8E (Lutter et al.,

[1]Department of Biotechnology, Bhupat and Jyoti Mehta School of Biosciences, Indian Institute of Technology Madras, Chennai 600036, Tamil Nadu, India. [2]CSIR Centre for Cellular and Molecular Biology, Hyderabad 500007, India.

*Author for correspondence (amal@iitm.ac.in)

A.K.B., 0000-0003-0362-5578

Received 6 March 2017; Accepted 25 September 2017

Journal of Cell Science

Journal of Cell Science (2017) 130, 3818-3828 doi:10.1242/jcs.203646

2017). VRAC currents have been biophysically characterized in *Xenopus* oocytes as well as in zebrafish, throwing light on the VRAC channel properties and heteromeric stoichiometry (Gaitán-Peñas et al., 2016; Yamada et al., 2016). Another recent article by Choi et al. revealed a link between VRAC and inflammation. Disruption of LRRC8A resulted in attenuation of TNF-induced inflammation by reducing superoxide production which, in turn, affected endocytosis of TNF receptors (TNFR1) (Choi et al., 2016).

Despite the significant participation of LRRC8 proteins in cellular events like T-lymphocyte development, B-cell maturation and reactive oxygen species (ROS)-mediated inflammation, the most persistent aspect of LRRC8 has been their channel-forming ability, initially strengthened by virtue of sharing evolutionary, structural and sequential relationship with channel-forming pannexins (Abascal and Zardoya, 2012; Choi et al., 2016; Kubota et al., 2004; Kumar et al., 2014; Sawada et al., 2003). Pannexins have been shown to participate in Ca^{2+} homeostasis by forming channels in the plasma membrane that release ATP (Bao et al., 2004). Extracellular ATP, in turn, increases intracellular Ca^{2+} through the activation of purinergic receptors. Additionally, pannexin 1 and 3 have been shown to form Ca^{2+}-permeable channels in the ER, thus contributing to Ca^{2+} leak from the endoplasmic reticulum (ER) stores (Ishikawa et al., 2011; Vanden Abeele et al., 2006). In light of considerable sequence similarity between pannexin and LRRC8B, and also based on the similar expression pattern of the two, we sought to determine whether the latter participates in Ca^{2+} homeostasis. Existing literature delineates the role of LRRC8A in VRAC formation and emphasizes that the channel functions in association with other subunits, most prominently LRRC8C–LRRC8E. In addition, disruption of LRRC8B fails to affect the transport of neuro-modulators via VRAC (Lutter et al., 2017). The absence of a noteworthy contribution of LRRC8B in the multimeric composition of VRAC, as well as transport, suggests the possibility that it has distinct activity on its own. Here, we found that overexpression of human LRRC8B in HEK293 cells attenuated the ATP-, carbachol- and thapsigargin (TG)-induced intracellular Ca^{2+} rise. It also increased the leak rate of ER Ca^{2+}, which was, by contrast, reduced following depletion of LRRC8B, suggesting it is a candidate as an ER Ca^{2+} leak channel. Moreover, LRRC8B did not affect the expression and function of LRRC8A.

This study is the first to denote one of the LRRC8 family proteins, LRRC8B, as a passive Ca^{2+} leak channel being localized in the ER. Participation of LRRC8B in a universal cellular phenomenon such as passive Ca^{2+} efflux from the ER may influence cellular physiology, dictating the filling and emptying status of the ER.

RESULTS

Overexpression of LRRC8B attenuates the IP_3 receptor-activated $[Ca^{2+}]_c$ rise

HEK293 cells were transfected with a plasmid containing full-length human *LRRC8B* cDNA. Overexpression of LRRC8B was validated by performing western blotting, as shown in Fig. 1A. Real-time PCR revealed that overexpression of LRRC8B did not alter the gene expression of other subtypes of LRRC8 (Fig. 1B). The ATP-induced rise of the cytosolic Ca^{2+} concentration $[Ca^{2+}]_c$ was compared between LRRC8B- and vector (control)-transfected HEK293 cells. In the presence of 1.8 mM Ca^{2+} in the extracellular fluid (ECF), application of 100 µM ATP elevated the $[Ca^{2+}]_c$ immediately. The ratio of fluorescence at 340 nm to that at 380 nm (a readout of the Ca^{2+} concentration as measured by Fura-2, denoted $F_{340/380}$) increased by 4-fold, from 1 to 4.1±0.07 (mean± s.e.m., n=120 cells) in control cells (Fig. 1C,E). Interestingly, the ATP-induced $[Ca^{2+}]_c$ rise in LRRC8B-transfected cells was significantly less compared to that in control cells (Fig. 1C,E). $F_{340/380}$ increased only ∼2.3 fold, from 1.3 to 3.05±0.1 (n=107). ATP is known to increase $[Ca^{2+}]_c$ by importing extracellular Ca^{2+} as well as by inducing release of Ca^{2+} from the ER via the phospholipase C (PLC) and inositol (1,4,5)-trisphosphate (IP_3) pathway. To check whether LRRC8B affected the Ca^{2+} influx or the release of Ca^{2+} from the ER stores, the experiment was performed in nominally Ca^{2+}-free ECF. The inhibitory effect of LRRC8B was noticed even in Ca^{2+}-free ECF (Fig. 1D,E). In control cells, the $F_{340/380}$ showed a 3-fold increase from 0.85 to 2.5±0.07 (n=72), whereas in LRRC8B-transfected cells the rise was 2-fold, which elevated from 0.9 to 1.9±0.04 (n=107). This suggests that LRRC8B affected Ca^{2+} release from the ER stores. To confirm this hypothesis further, we activated IP_3 receptors (IP_3Rs) directly by injecting IP_3 in cells through a patch pipette. Pipette solution containing 50 µM IP_3 raised the $F_{340/380}$ of Fura 2-loaded cells (bathed in Ca^{2+}-free ECF) immediately after 'whole cell' formation (Fig. S1A,B). Such a rise in the $[Ca^{2+}]_c$ was observed only when pipette solution contained IP_3. As expected, LRRC8B-overexpressing cells exhibited lesser rise of Ca^{2+} compared to the vector-transfected control cells. Furthermore, we checked whether the effect of LRRC8B is agonist dependent. $[Ca^{2+}]_c$ was elevated by activating muscarinic receptor with carbachol (100 µM). Like ATP, the carbachol-induced rise of $[Ca^{2+}]_c$ was attenuated significantly in LRRC8B-overexpressing cells (Fig. 1C,D).

Next, we uncoupled the ATP-mediated influx of extracellular Ca^{2+} from ER release by blocking IP_3R with two different blockers, 2-aminoethyl diphenylborate (2-APB) and xestospongin c. Cells were incubated with 50 µM 2-APB for 10–12 min before application of ATP. In Ca^{2+}-free ECF, ATP did not cause an elevation in $[Ca^{2+}]_c$ in 2-APB-treated cells, suggesting the effective blocking of Ca^{2+} release from the ER (Fig. 2A). As with 2-APB, xestospongin c-treated cells (3 µM for 10-12 min) did not show any ATP-induced $[Ca^{2+}]_c$ rise, confirming efficient blocking of IP_3R (Fig. 2B). The ATP-induced $[Ca^{2+}]_c$ rises were compared among control, LRRC8B-overexpressing and -knockdown cells after blocking IP_3R with 2-APB and xestospongin c. In the presence of 1.8 mM extracellular Ca^{2+}, ATP increased $[Ca^{2+}]_c$ in all groups to the same extent (Fig. 2C–F) suggesting that LRRC8B does not influence the ATP-induced influx of extracellular Ca^{2+}. Under xestospongin c treatment, the fold changes in Ca^{2+} rise in response to ATP in 1.8 mM Ca^{2+}, recorded were 2.3±0.2, 2.2±0.2, 2.3±0.2 and 2.0±0.1 in control, overexpressing, scrambled-transfected and knockdown cells (n=12–14), respectively. Similarly, in the case of 2-APB treatment, ATP in the presence of 1.8 mM Ca^{2+} gave rise to fold increases of 2.3±0.1, 2.2±0.1, 2.5±0.05 and 2.5±0.07 in $[Ca^{2+}]_c$ in control, overexpressing, scrambled-transfected and knockdown cells (n=22–24), respectively.

The above-mentioned results, particularly those shown in Fig. 2A, may arise from the off-target promiscuity and multiple effects of 2-APB. Depending on its concentration and incubation time, 2-APB may deplete ER Ca^{2+} stores by activating IP_3R (Ma et al., 2002). If 2-APB treatment indeed depleted the stores, in this case, ATP would not release any Ca^{2+} from ER. Therefore, the results shown in Fig. 2A could be a reflection of 'empty ER stores' due to IP_3R activation rather than its inhibition by 2-APB. We checked the ER Ca^{2+} status following 2-APB treatment (Fig. S2A). Ionomycin (5 µM) was added in Ca^{2+}-free ECF after 2-APB treatment to access the Ca^{2+} content of the ER store. The ionomycin-induced $[Ca^{2+}]_c$ rise in 2-APB-treated cells was comparable

Journal of Cell Science (2017) 130, 3818-3828 doi:10.1242/jcs.203646

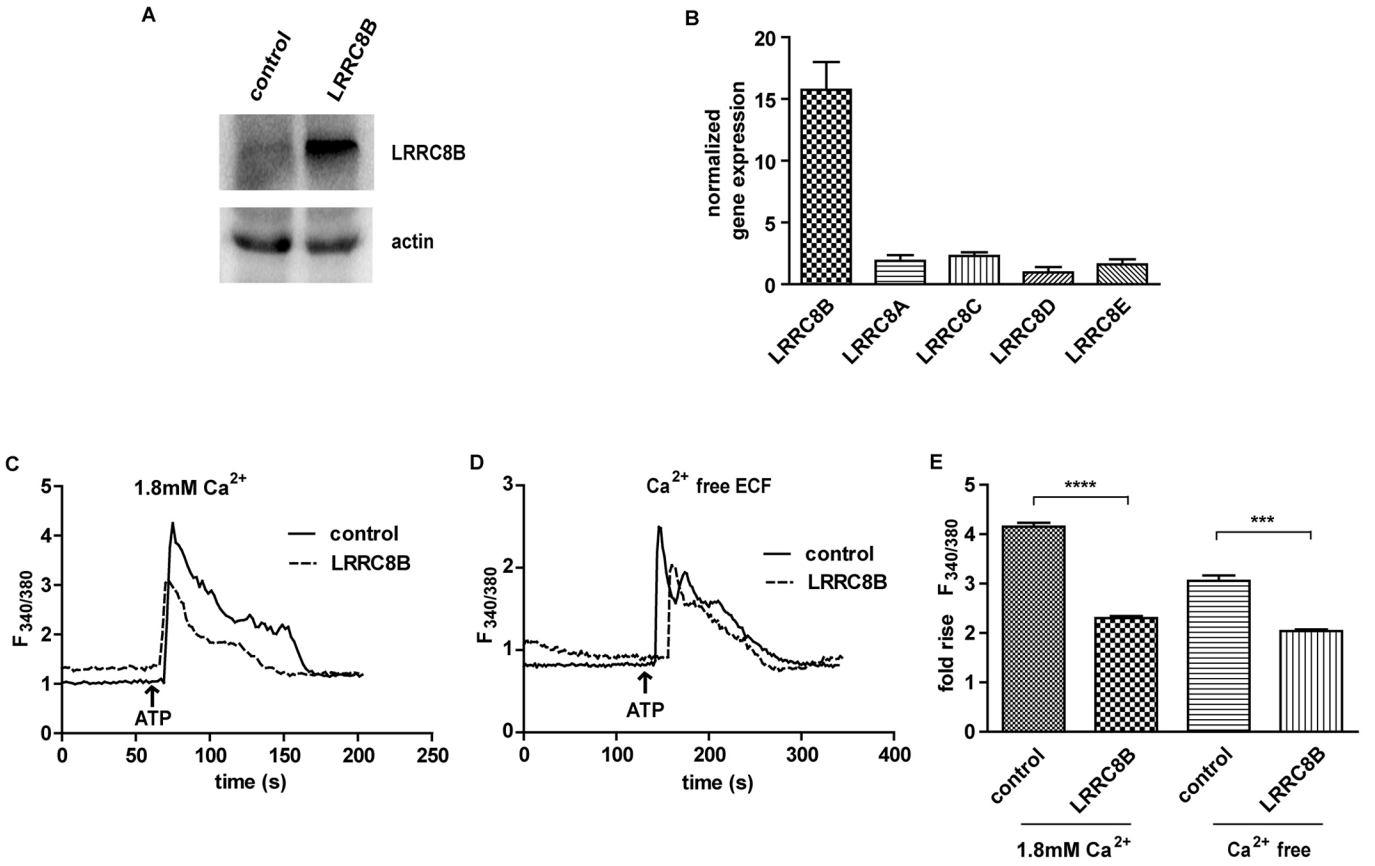

Fig. 1. Overexpression of LRRC8B attenuates the ATP-induced $[Ca^{2+}]_c$ rise. (A) Western blot showing the overexpression of LRRC8B in HEK293 cells following transient transfection. β-actin was used as a loading control. (B) Quantitative PCR reveals an increase of LRRC8B gene expression in the transfected cells, but no significant changes in expression of other LRRC8 subtypes. The fold changes in mRNA expression in LRRC8B-overexpressing cells have been plotted with respect to control cells, normalized to β-actin. (C) Ca^{2+} transients elicited by 100 µM ATP (in presence of 1.8 mM extracellular Ca^{2+}) in control and LRRC8B-transfected HEK293 cells. LRRC8B-transfected cells showed a lower rise. (D) Representative traces of the $[Ca^{2+}]_c$ rise induced by the application of 100 µM ATP in nominally Ca^{2+}-free external buffer. LRRC8B-mediated inhibition is also evident in the absence of external Ca^{2+}. (E) The fold rise of $F_{340/380}$, representing the ATP-induced $[Ca^{2+}]_c$ rise, is shown. The ATP-induced $[Ca^{2+}]_c$ rise, both in the presence and absence of extracellular Ca^{2+} in LRRC8B-transfected cells is significantly lower than in vector-transfected control cells. Values are the mean±s.e.m. of 72–120 cells. ***$P\leq0.001$; ****$P\leq0.0001$.

with that in the untreated control cells. The $F_{340/380}$ was increased by 11-fold in untreated cells and 13-fold in 2-APB-treated cells ensuring that 2-APB treatment did not deplete the ER Ca^{2+} store. Furthermore, the ER Ca^{2+} was measured directly by using ER-targeted R-CEPIA1er, a Ca^{2+}-sensitive fluorescent protein (Suzuki et al., 2014). As shown in Fig. S2B–D, neither 2-APB nor xestospongin c altered the ER Ca^{2+} level. The basal fluorescence intensity in the ER showed no difference following 2-APB and xestospongin c treatment (Fig. S2B). ATP treatment caused a decay in fluorescence intensity in control cells but not in 2-APB- and xestospongin c-treated cells (Fig. S2C,D). Taken together, it confirms that in our experimental conditions 2-APB and xestospongin c specifically blocked IP_3R and did not alter the level of Ca^{2+} in the ER.

We examined whether LRRC8A has a similar influence on Ca^{2+} signaling, like LRRC8B. As shown in Fig. S3, neither overexpression nor knockdown of LRRC8A had any effect on ATP-induced $[Ca^{2+}]_c$ rise in Ca^{2+}-free ECF.

LRRC8B alters the releasable Ca^{2+} pool in the ER

Next, we explored the effect of LRRC8B on the concentration of Ca^{2+} in the ER ($[Ca^{2+}]_{ER}$). To find out whether LRRC8B altered the amount of releasable Ca^{2+} in the ER, we examined the effects of thapsigargin (TG), a sarco-endoplasmic reticulum Ca^{2+}-ATPase (SERCA) pump blocker. Application of 1 µM TG in nominally Ca^{2+}-free ECF, led to a slow increase in $[Ca^{2+}]_c$ both in vector-(control) and LRRC8B-transfected cells (Fig. 3A). However, LRRC8B-overexpressing cells had a significantly lower rise of $[Ca^{2+}]_c$ compared to that in the control cells. The fold increases in $F_{340/380}$ were 1.9±0.08 (n=39) and 1.5±0.05 (n=45) in control- and LRRC8B-transfected cells, respectively (Fig. 3A,B). This implies that the amount of releasable Ca^{2+} in LRRC8B-overexpressing cells is possibly lower than that of control cells. Furthermore, we suppressed the expression of endogenous LRRC8B by using siRNA. Scrambled siRNA was used as a control. 50 nM of siRNA reduced the expression of LRRC8B but not the endogenous level of LRRC8A and β-actin, as detected by western blotting (Fig. 3C). LRRC8B-knockdown cells exhibited a significantly higher TG-induced $[Ca^{2+}]_c$ rise, compared to the scrambled siRNA-transfected cells (Fig. 3A,B). There was a 1.73±0.08-fold increase in $F_{340/380}$ in scrambled-transfected cells (n=29), whereas the increase was 2.1± 0.07-fold in LRRC8B-knockdown cells (n=45).

The above experiments indicate that Ca^{2+} content in the ER stores is diminished as a result of LRRC8B overexpression. To check this further, we estimated the ER Ca^{2+} pool size in control and LRRC8B-overexpressing cells by applying ionomycin (5 µM) in Ca^{2+}-free ECF. As shown in Fig. 3D,E, ionomycin treatment caused a significantly lower rise of $[Ca^{2+}]_c$ in LRRC8B-

Journal of Cell Science (2017) 130, 3818-3828 doi:10.1242/jcs.203646

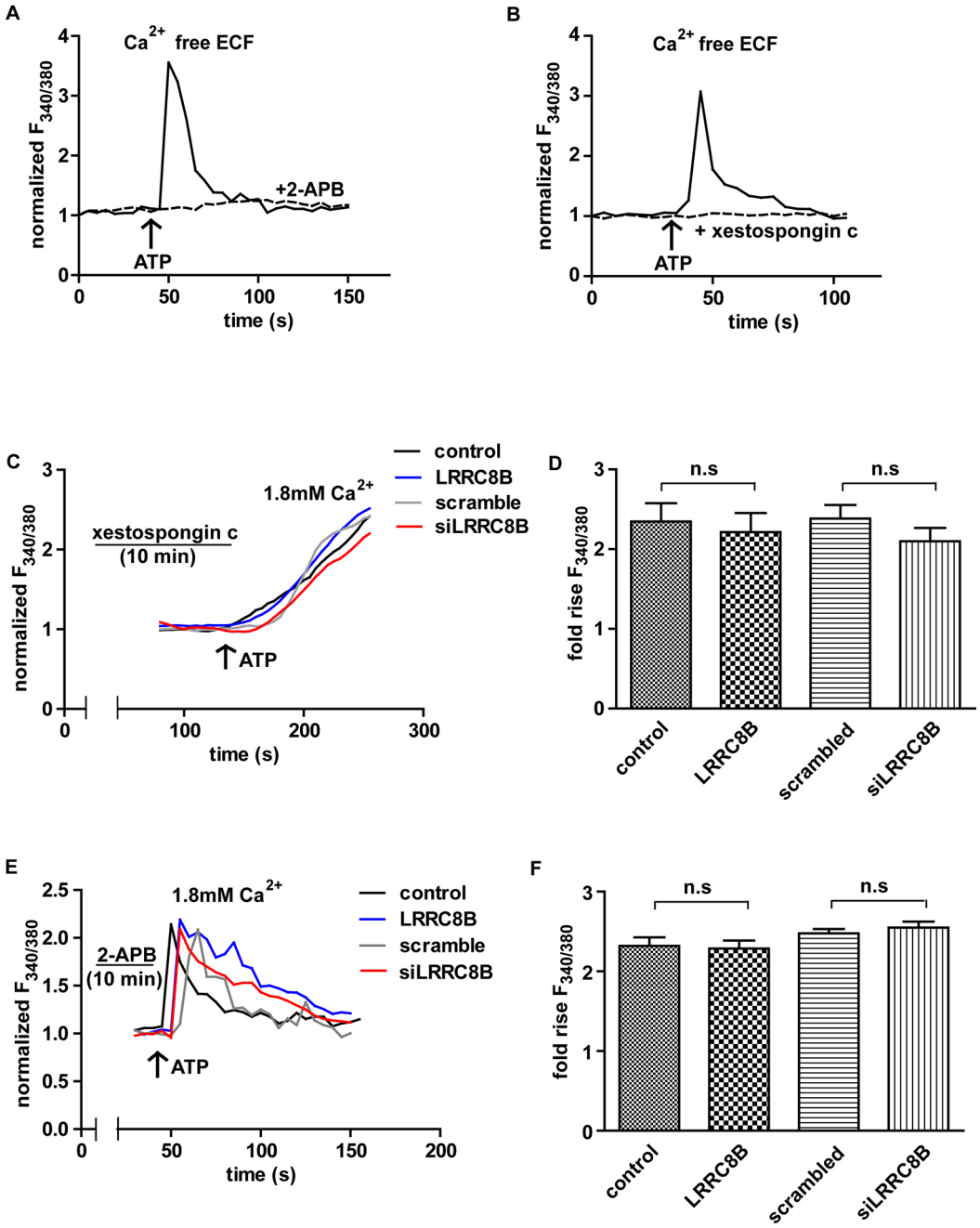

Fig. 2. LRRC8B does not affect the ATP-induced influx of extracellular Ca^{2+}. (A,B) The ATP-induced $[Ca^{2+}]_c$ rise in control (solid line) and 2-APB- or xestospongin c-treated cells (broken line) is shown. Ca^{2+}-free ECF was used. The IP_3R blockers 2-APB (50 µM) and xestospongin c (3 µM) blocked the $[Ca^{2+}]_c$ rise completely. (C) In the presence of 1.8 mM Ca^{2+} in ECF, xestospongin c (3 µM)-treated control as well as LRRC8B-overexpressing and -knockdown (siLRRC8B) cells exhibited the same extent of ATP-induced $[Ca^{2+}]_c$ rise. Scramble, scrambled siRNA. (D) Bar diagram depicts the cumulative data from experiments as in C for 12–14 cells. Values are the mean±s.e.m. (E) The ATP-induced $[Ca^{2+}]_c$ rise (in 1.8 mM Ca^{2+} containing ECF) exhibited by 2-APB-treated control, and LRRC8B-overexpressing and -knockdown cells. All the groups showed the same extent of $[Ca^{2+}]_c$ rise. (F) Results from experiments as in E (mean± s.e.m. from 22–24 cells). Cells were first incubated with the blocker for 10–12 min, followed by the application of ATP (100 µM). n.s, not significant, $P>0.05$ (Student's *t*-test).

overexpressing cells. $F_{340/380}$ was increased by 11±0.8-fold (n=52) in control cells, whereas the increase was 7±0.4 fold (n=44) in overexpressing cells.

LRRC8B is involved in ER Ca^{2+} leak

The role of LRRC8B in ER Ca^{2+} was probed further by measuring $[Ca^{2+}]_{ER}$ with ER-targeted red fluorescent protein RCEPIA1er and Mag-Fura-2 (Suzuki et al., 2014). Results obtained using RCEPIA1er are shown in Fig. 4, while $[Ca^{2+}]_{ER}$ measured via Mag-Fura-2 is presented in Fig. S4. In order to estimate the leakage of Ca^{2+} from the ER, the SERCA pump was blocked with TG, rendering the Ca^{2+} flow unidirectional (i.e. from the ER to the cytosol). Blocking of the SERCA pump resulted in a gradual decrease in $[Ca^{2+}]_{ER}$ brought about by leak channels in the ER (Fig. 4A). Interestingly, LRRC8B-overexpressing cells exhibited a faster decay in $[Ca^{2+}]_{ER}$, whereas its knockdown decelerated the reduction in $[Ca^{2+}]_{ER}$. The initial

Journal of Cell Science (2017) 130, 3818-3828 doi:10.1242/jcs.203646

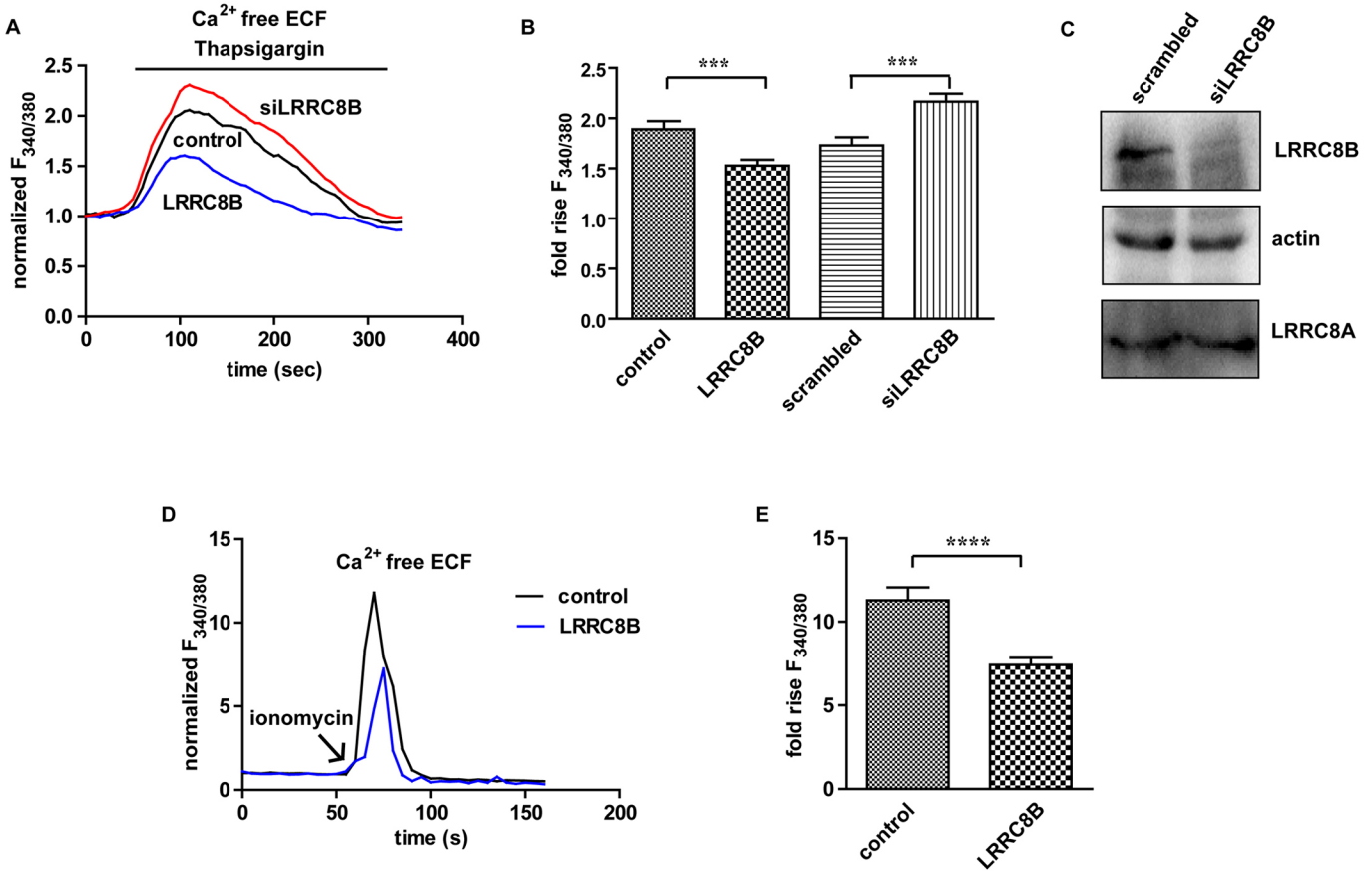

Fig. 3. LRRC8B regulates the ER Ca^{2+} pool. (A) Representative traces showing the increase in $[Ca^{2+}]_c$ in HEK293 cells in response to 1 µM TG in nominally Ca^{2+}-free extracellular solution. Cells overexpressing LRRC8B showed a lower TG-mediated $[Ca^{2+}]_c$ rise compared to the control, whereas it was higher in LRRC8B-knockdown cells (siLRRC8B). (B) Graph of data for experiments as in A showing the fold rise of $[Ca^{2+}]_c$ evoked by 1 µM TG. Values are the mean±s.e.m. for 20–40 cells. ***$P\leq0.001$. (C) Western blot showing the siRNA (50 nM)-mediated knockdown of endogenous LRRC8B expression in HEK293 cells. β-actin was used as an internal control. The expression level of LRRC8A was not affected. (D) Representative $[Ca^{2+}]_c$ transients elicited by 5 µM ionomycin in control and LRRC8B-overexpressing cells. The experiment was performed in Ca^{2+}-free ECF. (E) Graph of data for experiments as in D showing the fold rise of $[Ca^{2+}]_c$ evoked by ionomycin, which is less when LRRC8B is overexpressed. Values are the mean±s.e.m. for 22–26 cells. ****$P\leq0.0001$.

fluorescence intensity before TG application (i.e. the basal level of $[Ca^{2+}]_{ER}$) was normalized to 100 and the percentage of fluorescence decrease in half of the total time duration ($t_{1/2}$) was estimated (TG was applied for 270 s). The higher the fluorescence reduction in $t_{1/2}$, the faster the Ca^{2+} leak is. In the case of control- and scrambled-transfected cells, the $t_{1/2}$ fluorescence decreased by 30±2% (mean±s.e.m.; n=54), whereas in LRRC8B-transfected cells it was 45±2% (n=42) and 16±1% (n=48) in case of knockdown cells (Fig. 4A,B). We compared the basal level of $[Ca^{2+}]_{ER}$ in LRRC8B-overexpressing and -knockdown cells. As shown in Fig. 4C, overexpression and knockdown of LRRC8B reduced and elevated $[Ca^{2+}]_{ER}$, respectively, supporting its connection to ER Ca^{2+} leak. The fluorescence intensities of control- and scrambled-transfected cells were 2564±113 (n=54) and 3450±158 (n=52) (arbitrary units), whereas in LRRC8B-overexpressing and -knockdown cells the values were 1782±114 (n=42) and 6014±514 (n=42), respectively. Furthermore, the effect of LRRC8B overexpression and knockdown on the expression of potential leak channel Bcl-2 was checked via western blotting (Bassik et al., 2004; Pinton et al., 2000). No notable difference was found, as shown in Fig. 4D.

Effect of LRRC8B on store-operated Ca^{2+} entry

Lowering of $[Ca^{2+}]_{ER}$ activates store-operated Ca^{2+} entry (SOCE). Therefore, the activation of LRRC8B is likely to promote SOCE. Overexpression of LRRC8B might be expected to cause a constitutive SOCE activation and thereby a rise in basal $[Ca^{2+}]_c$ level. As shown in Fig. 5A, the basal $[Ca^{2+}]_c$ in LRRC8B-overexpressing cells was found to be slightly higher than control. The $F_{340/380}$ recorded in LRRC8B-overexpressing cells was 1.6±0.04 (n=74) compared to 1.1±0.04 (n=72) in control cells. Although the difference is not huge, it was found to be statistically significant. However, knocking down of endogenous LRRC8B did not change the level of basal $[Ca^{2+}]_c$ (Fig. 5A). We examined SOCE in LRRC8B-overexpressing and -knockdown cells. Cells were treated with 1 µM TG in nominally Ca^{2+}-free ECF for ∼5 min to deplete the stores. After TG treatment, cells were replenished with ECF containing 1.8 mM Ca^{2+} resulting in a robust rise of $[Ca^{2+}]_c$ as a result of SOCE activation (Fig. 5B). As depicted in Fig. 5B,C, the $[Ca^{2+}]_c$ rise caused by SOCE activation was significantly higher in LRRC8B-overexpressing cells, which showed an $F_{340/380}$ to 4.2±0.17 fold (n=77) as compared to 3.2±0.16 fold (n=69) in control cells. However, no significant difference was noted between scrambled-transfected and LRRC8B-knockdown cells. We estimated the residual Ca^{2+} in the ER after 5 min of TG treatment. A representative experiment is shown in Fig. 4A. The fluorescence intensity of RCEPIA1er before the application of TG was normalized to 100%. The residual fluorescence was compared between control, overexpressing and knockdown cells. It was 54±

Journal of Cell Science (2017) 130, 3818-3828 doi:10.1242/jcs.203646

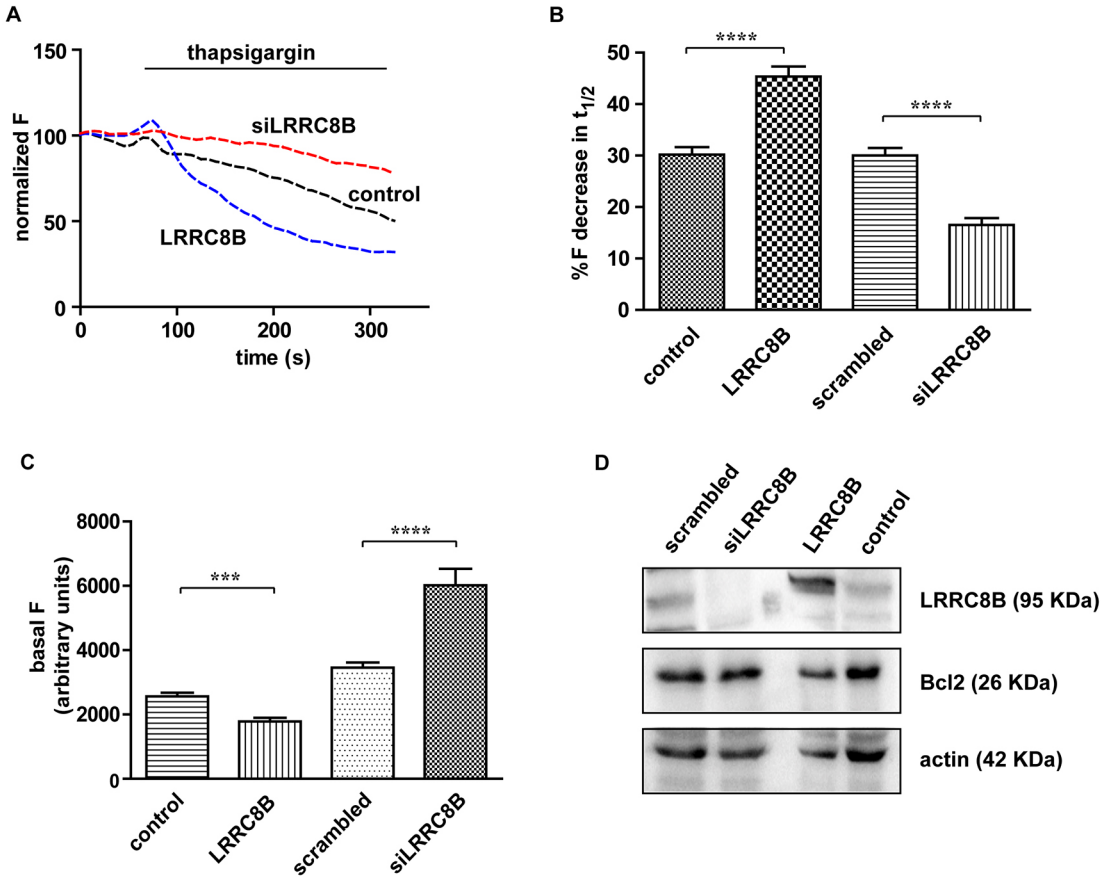

Fig. 4. LRRC8B enhances the rate of a passive Ca^{2+} leak from the ER. (A) Representative traces showing the decay of luminal Ca^{2+} ($[Ca^{2+}]_{ER}$), upon blocking the SERCA pump with 1 µM TG. The normalized fluorescence of the ER-targeted Ca^{2+} indicator RCEPIA1er is shown. Cells expressing RCEPIA1er alone (labeled control) are considered as a control for overexpression studies and those expressing RCEPIA1er along with scrambled siRNA are regarded as a control for knockdown studies (siLRRC8B). (B) Graph of data for experiments as in A (mean±s.e.m., n=42–54) for the decrease in percentage fluorescence (F) in $t_{1/2}$. (C) Fluorescence intensities in the basal state (before TG application, at time zero) showing that there is a lower $[Ca^{2+}]_{ER}$ in LRRC8B-overexpressing cells and, contrastingly, a higher $[Ca^{2+}]_{ER}$ in cells subjected to LRRC8B knockdown, compared to the control cells. Values are mean±s.e.m. (n=42-54). (D) Western blot showing no significant change in expression status of the known leak channel Bcl-2 upon LRRC8B overexpression and knockdown. ***P≤0.001; ****P≤0.0001.

1% (n=41) in control cells as opposed to 36±1% (n=82) in LRRC8B-overexpressing cells and 56±2% (n=28) in scramble-transfected cells in comparison to 65±2% (n=40) in siRNA-transfected cells (Fig. 5D). This indicates that the diminished level of residual Ca^{2+} in the ER following TG treatment in LRRC8B-overexpressing cells could be the basis of the higher SOCE in these cells. Collectively, these results suggest that LRRC8B is associated with the Ca^{2+} leak from the ER with a regulatory effect on SOCE.

Localization of LRRC8B

HEK293 cells were transfected with LRRC8B–GFP (~400 ng/ml) and the localization of expressed protein was analyzed by using confocal microscopy. Cells were stained with the ER-specific marker ER-Tracker Red. Fig. 6A shows the overlay of GFP and ER-Tracker Red images, suggesting colocalization (yellow). The degree of colocalization was quantified by using ImageJ Fiji software on background-subtracted images, which yielded an average Pearson's correlation coefficient of 0.61, indicating a good association between the distribution of LRRC8B and ER. To rule out the possibility of retention of LRRC8B in the ER due to overexpression, the presence of endogenous LRRC8B was checked in the ER and other subcellular fractions by western blotting (Fig. 6B). Membrane protein connexin 43 (also known as GJA1) was used as a plasma membrane marker, while PARP was used for the nucleus. VDAC was used as a marker for mitochondria, and chaperone protein ERp72 (also known as PDIA4) was used as an ER marker. Endogenous LRRC8B was mostly identified in the ER fraction along with traces in the mitochondria, but not in the plasma membrane or cytosolic fraction. Moreover, LRRC8A was found only in the membrane fraction, as validated in the literature (Qiu et al., 2014; Voss et al., 2014; Fig. 6C).

LRRC8B does not affect the function of LRRC8A

Overexpression and knockdown of LRRC8B did not affect the expression of LRRC8A (Figs 1B and 3C). Furthermore, we checked whether LRRC8B affects the VRAC function of LRRC8A, by performing a specific YFP-quenching assay (Qiu et al., 2014; Voss et al., 2014). A halide-sensitive mutant YFP was used as a reporter of VRAC function (Galietta et al., 2001). A hypotonic stimulus promoted the movement of halide into the cells through activated VRAC, composed of LRRC8A, resulting in cell swelling and YFP quenching. On application of NaI, hypotonicity-induced YFP quenching was observed, which was inhibited by the VRAC blocker DCPIB (50 µM) (Fig. 7A). Furthermore, knocking down of LRRC8A attenuated the YFP quenching significantly (Fig. 7A,C). In the case of control, normalized fluorescence decreased to 33±1 (n=31) in 5 min, whereas in LRRC8A-knockdown cells this value was 63±2 (n=19), confirming LRRC8A involvement in VRAC

Journal of Cell Science (2017) 130, 3818-3828 doi:10.1242/jcs.203646

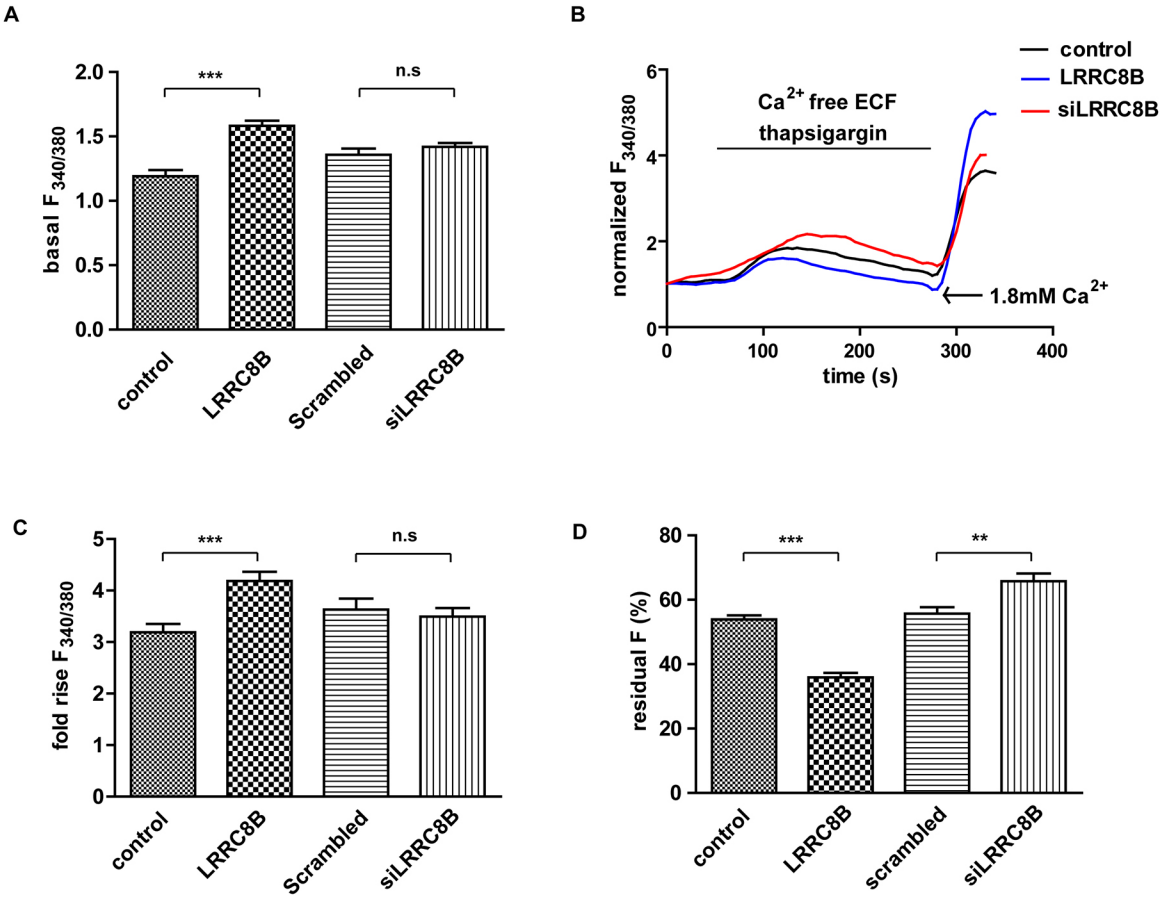

Fig. 5. LRRC8B modulates SOCE. (A) Graph of data for experiments measuring the $F_{340/380}$, reflecting the basal $[Ca^{2+}]_c$, in control, LRRC8B-overexpressing, scrambled-transfected and knockdown cells (siLRRC8B). Basal $[Ca^{2+}]_c$ in LRRC8B-overexpressing cells is significantly higher than in control. Values are the mean±s.e.m. for n=33–72 cells. (B) Representative traces showing the SOCE. ER Ca^{2+} stores were depleted upon treatment with 1 µM TG in nominally Ca^{2+}-free ECF, resulting in a rise of $[Ca^{2+}]_c$ (first peak; shown in more detail in Fig. 3). The second Ca^{2+}-transient peak observed following the addition of 1.8 mM Ca^{2+} containing ECF reflects SOCE. (C) Graph of data for experiments measuring the fold changes in $[Ca^{2+}]_c$ as a result of SOCE (second peak in B) under differential expression of LRRC8B. Cells with overexpression of LRRC8B showed a higher SOCE. Values are the mean±s.e.m. of 30–47 cells. (D) Residual $[Ca^{2+}]_{ER}$ after 300 s of TG treatment. Cells were transfected with ER-targeted RCEPIA1er, with or without LRRC8B and its siRNA. ER Ca^{2+} was imaged before and after 300 s of incubation with TG (in Ca^{2+}-free ECF). The residual percentage fluorescence (F) was calculated as (F_{300s}×100)/F_0, where F_0 is the initial fluorescence and F_{300s} is the fluorescence after 300 s of TG application. Values are the mean±s.e.m. for 30–45 cells. $^{**}P \leq 0.01$; $^{***}P \leq 0.001$; n.s., not significant.

formation. Interestingly, when LRRC8B was overexpressed or depleted, hypotonicity-induced VRAC activation was not affected. As shown in Fig. 7B,C, both in LRRC8B-overexpressing and -knockdown cells, the fluorescence reduced to the same extent. This result confirms that LRRC8B does not alter the function of LRRC8A.

DISCUSSION

On account of a close evolutionary relationship with pannexin and the presence of conserved motifs in the transmembrane helices, LRRC8 proteins were proposed to form a hexameric channel (Abascal and Zardoya, 2012). Later studies showed that there was an association of LRRC8A with VRAC (Qiu et al., 2014; Voss et al., 2014). In this study, we found that ATP-induced elevation of $[Ca^{2+}]_c$ was lower in LRRC8B-overexpressing cells. The inhibitory effect of LRRC8B was detected even in the absence of extracellular Ca^{2+}. This observation led us to assume that LRRC8B exerts its effect by modulating the release of Ca^{2+} from the ER, rather than by affecting the ATP-induced influx of Ca^{2+} from the extracellular space. When the IP_3-induced release of ER Ca^{2+} was blocked by 2-APB and xestospongin c, in presence of extracellular Ca^{2+}, the ATP-mediated $[Ca^{2+}]_c$ rise remained the same as in the control for both in LRRC8B-overexpressing and -knockdown cells, confirming that LRRC8B does not affect the ATP-induced entry of extracellular Ca^{2+}. In the same line, the effect of LRRC8B on ER Ca^{2+} release became apparent when IP_3Rs were directly activated by injecting IP_3 or through activating muscarinic receptor with carbachol. In Ca^{2+}-free ECF, LRRC8B-overexpressing cells exhibited a lower $[Ca^{2+}]_c$ rise upon stimulation with either IP_3 or carbachol (Fig. S1) than did control cells.

The impaired rise of $[Ca^{2+}]_c$ due to LRRC8B overexpression could be a reflection of the ER Ca^{2+} status. Thus, we measured the TG-releasable ER Ca^{2+} pool. It was lower in LRRC8B-overexpressing cells and higher in LRRC8B-knockdown cells (Fig. 3A,B). If LRRC8B positively modulated the plasma membrane Ca^{2+} ATPase (PMCA) that pumps out $[Ca^{2+}]_c$, one would expect the same result (i.e. the TG-induced $[Ca^{2+}]_c$ rise would be lower in LRRC8B-overexpressing cells and more in the case of LRRC8B knockdown). To rule out this possibility, we followed the Ca^{2+}- leak from the ER as well as measuring its Ca^{2+} content by using direct and indirect methods. Estimation of ER Ca^{2+} pool size with a high dose of ionomycin revealed that there was a lower ER Ca^{2+} content in LRRC8B-overexpressing cells (Fig. 3D,E). Direct measurement of ER Ca^{2+} levels with ER-targeted R-CEPIA1er also showed that overexpression and knockdown of LRRC8B decreased and

Journal of Cell Science (2017) 130, 3818-3828 doi:10.1242/jcs.203646

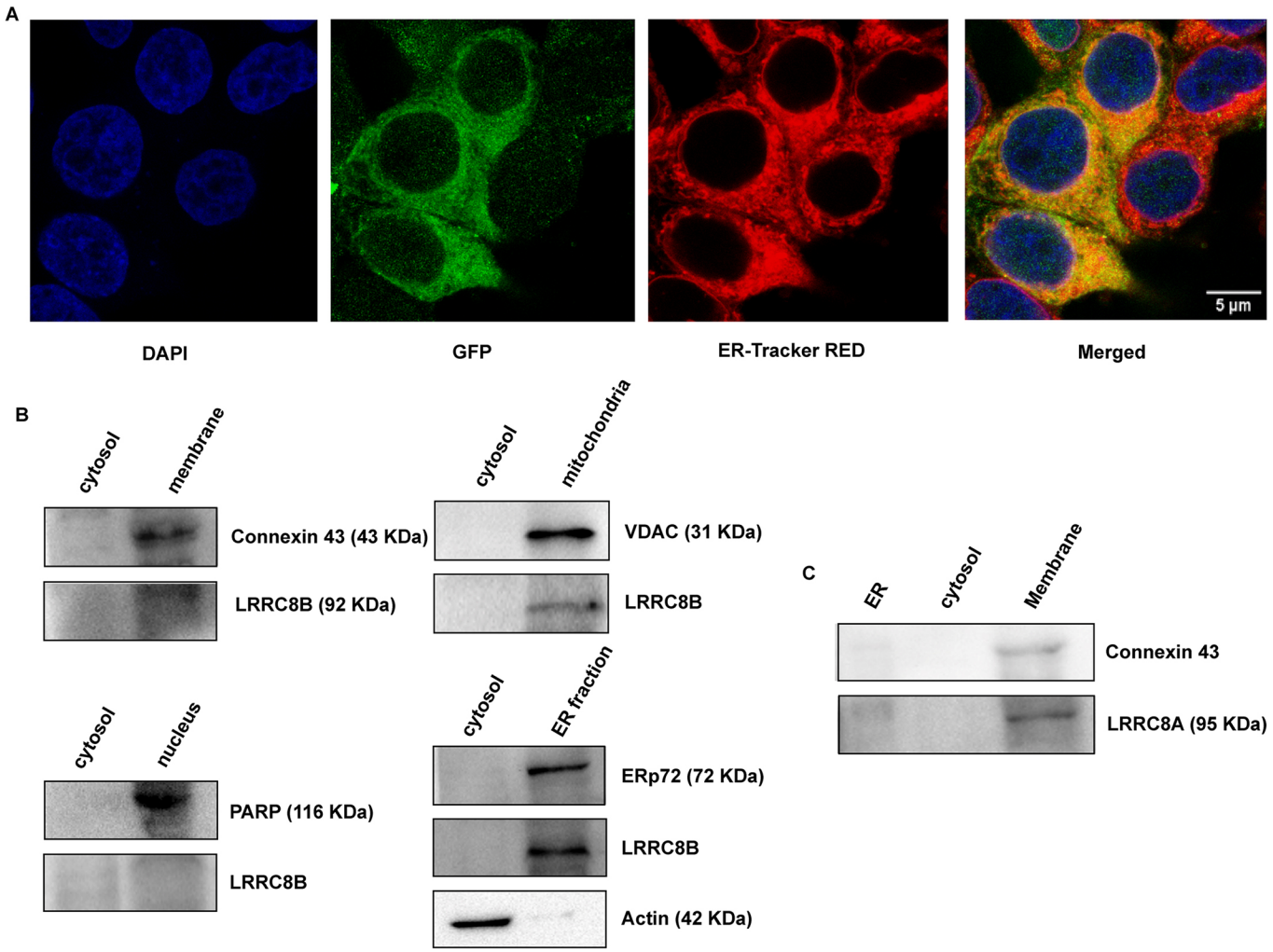

Fig. 6. Cellular localization of LRRC8B. (A) Confocal microscopy images showing the localization of overexpressed LRRC8B in the ER. LRRC8B–GFP-expressing cells were stained with the ER-specific dye ER-Tracker Red. Nuclei were stained with DAPI. An overlay of GFP and ER-Tracker Red fluorescence showed co-localization (yellow) of LRRC8B with the ER. (B) Western blot showing the presence of endogenous LRRC8B in the ER-enriched cellular fraction. In addition, trace amounts of LRRC8B were found in mitochondria but not in the plasma membrane and nuclear fractions. Cellular fractionation was validated with respective marker proteins (ERp72 for ER, connexin 43 for plasma membrane, VDAC for mitochondria and PARP for the nucleus). (C) Western blot showing the presence of endogenous LRRC8A in the plasma membrane fraction with no traces in ER and cytosol.

increased the basal level of $[Ca^{2+}]_{ER}$, respectively (Fig. 4C). The rate of Ca^{2+} leak from the ER was measured after blocking the SERCA pump with TG, and we found that LRRC8B-transfected cells showed a faster $[Ca^{2+}]_{ER}$ leak whereas its depletion made it slower (Fig. 4A,B), strengthening the possibility that LRRC8B is a potential leak channel. Although, the modulation of the PMCA by LRRC8B has not been detected in our experimental condition, the possibility still remains. LRRC8B might modulate PMCA as well as some other members of the Ca^{2+} signaling network, which needs further investigation and different experimental strategies.

If LRRC8B negatively modulated the IP_3R, it would also be expected that the $[Ca^{2+}]_c$ rise induced by ATP, IP_3 and carbachol would be attenuated in LRRC8B-overexpressing cells. However, such a hypothesis does not explain the IP_3R-independent changes observed, such as the a change in TG-induced $[Ca^{2+}]_c$ rise or altered leak rate of $[Ca^{2+}]_{ER}$, in response to the manipulation of the LRRC8B level.

The obvious question that arises is if LRRC8B brings down the $[Ca^{2+}]_{ER}$, does it also activate SOCE. Interestingly, the basal level of $[Ca^{2+}]_c$ in LRRC8B-overexpressing cells was found to be higher (Fig. 5A), an indication of the constitutive SOCE activation. The SOCE after ER store depletion with TG was found to be higher in LRRC8B-overexpressing cells (Fig. 5B,C). The faster leakage of ER Ca^{2+} following TG treatment in the LRRC8B-overexpressing cells, resulted in a lower residual $[Ca^{2+}]_{ER}$ (Fig. 5D). As the stores are relatively more empty, SOCE observed in LRRC8B-overexpressing cells is significantly higher (Fig. 5B,C) compared to in the control cells. Interestingly, although LRRC8B-knockdown cells exhibited a higher residual $[Ca^{2+}]_{ER}$ compared to the respective scrambled siRNA-transfected control, it did not have any impact on SOCE (Fig. 5B–D). Possibly, the difference in residual $[Ca^{2+}]_{ER}$ between knockdown and mock-transfected cells was not enough to result in a significant change in SOCE.

In addition, both LRRC8B-GFP and endogenous LRRC8B were found to be localized in the ER, reinforcing the potential role of LRRC8B in ER Ca^{2+} leak. Overexpression or knockdown of LRRC8B affected neither the expression nor the function of LRRC8A (Figs 1B, 3C and 7). Similarly, overexpression or knockdown of LRRC8A did not bring about any change in the ATP-induced release of Ca^{2+} from the stores (Fig. S3) suggesting a distinct role for LRRC8B that does not

Journal of Cell Science (2017) 130, 3818-3828 doi:10.1242/jcs.203646

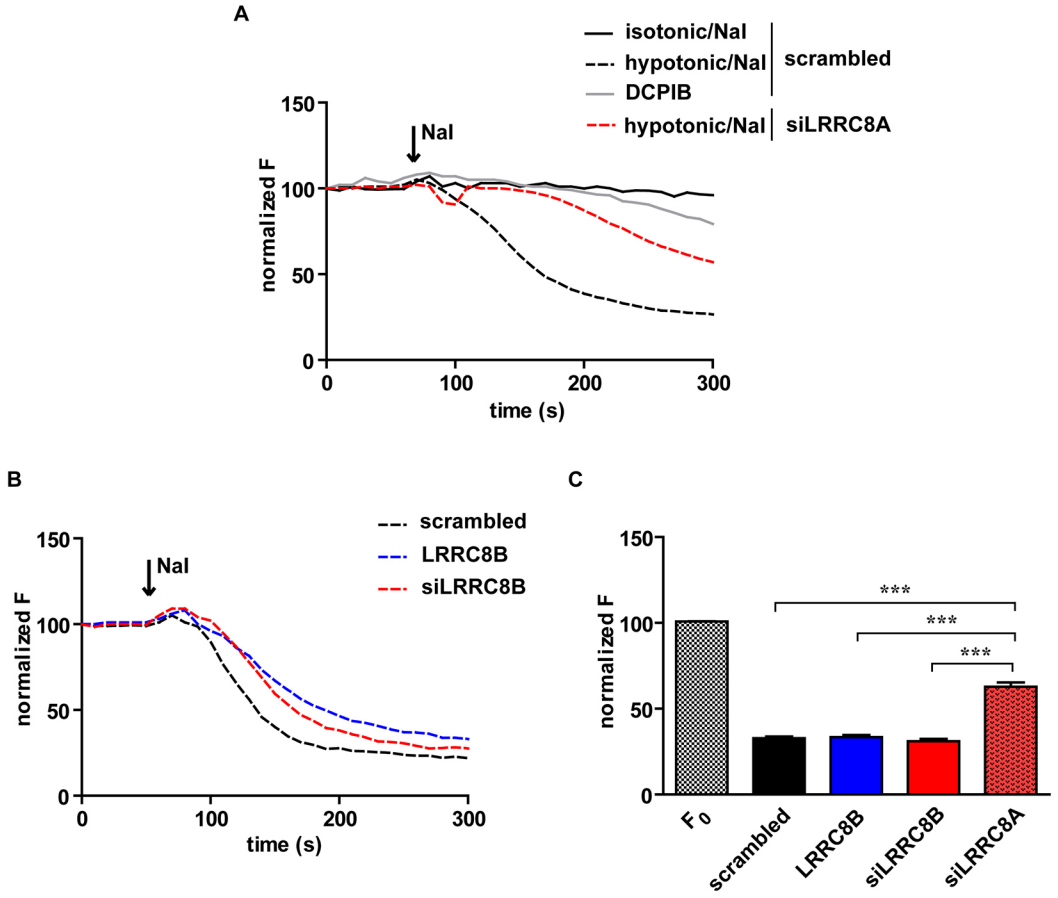

Fig. 7. LRRC8B does not affect LRRC8A-mediated VRAC function. (A) Representative traces showing YFP quenching under isotonic and hypotonic conditions upon addition of 50 mM NaI. Attenuation of the fluorescence intensity reflects the activation of the VRAC. Cells were transfected with halide-sensitive mutant YFP. Under the isotonic condition, no notable change in fluorescence was observed, whereas, in a hypotonic solution, the fluorescence decayed in control cells. Depletion of LRRC8A with siRNA (siLRR8A) or treatment with DCPIB, a chemical blocker of VRAC inhibited VRAC activation, as evident by the significant reduction in YFP quenching. (B) Overexpression (blue) and knockdown (red) of LRRC8B had no noticeable effect on VRAC-mediated YFP quenching in response to NaI under hypotonic challenge. (C) Graph of data for experiments as in B showing hypotonicity-induced VRAC activation under different conditions. Unlike with LRRC8A, manipulation of the level of LRRC8B did not affect the YFP quenching (VRAC activation). The initial fluorescence (F_0) was set at 100, and other results are normalized to this level. In LRRC8A-knockdown cells there was a ~37% reduction of fluorescence in 5 mins, whereas the reduction was ~70% in control as well as LRRC8B-overexpressing and -knockdown cells. Values are the mean±s.e.m. for 24–39 cells. ***$P \leq 0.001$.

affect VRAC-function and no significant contribution of LRRC8A in the leak channel function of LRRC8B.

The ER is the principal intracellular Ca^{2+} store and the Ca^{2+}-filling status of ER dictates essential cellular processes such as cell death, proliferation, gene expression etc. (Berridge et al., 2003; Clapham, 2007). A coordinated interplay between active Ca^{2+} uptake into the ER via the SERCA pump and passive release of Ca^{2+} by leak channels regulate the steady-state $[Ca^{2+}]_{ER}$ under normal conditions. SOCE is a universal Ca^{2+} influx mechanism that results from the depletion of ER Ca^{2+} stores followed by the activation of Ca^{2+} channels in the plasma membrane. Activation of SOCE results in a rise of $[Ca^{2+}]_c$ and subsequent refilling of the ER Ca^{2+} stores, resulting in regulation of ER Ca^{2+} homeostasis (Fierro and Parekh, 2000; Hofer et al., 1998). An earlier study has shown that IP_3Rs and ryanodine receptors (RyRs) do not participate in the basal ER Ca^{2+} leak, leaving the job to the leak channels of which very little has been known to date (Camello et al., 2002). Because the ER is the seat of protein translation and quality control, alterations in Ca^{2+} homeostasis can bring about ER stress leading to the unfolded protein response (UPR) and cell death (Hammadi et al., 2013). In addition, a firm control of $[Ca^{2+}]_{ER}$ has been shown to be significant in proper protein folding and cell survival (Sammels et al., 2010; Xu et al., 2005). A few of the proposed candidates for ER Ca^{2+} leak proteins are: (1) translocon channels modulating ER stress, (2) the anti-apoptotic protein Bcl-2, which brings upon a cell survival strategy through formation of a leak channel, (3) presenilins, whose loss of function as ER leak channels have been reported in familial Alzheimer's disease condition and (4) TMCO1, which has been recently identified as an ER-resident Ca^{2+} channel that prevents overfilling of stores (Amer et al., 2009; Brunello et al., 2009; Hammadi et al., 2013; Pinton et al., 2000; Tu et al., 2006; Van Coppenolle et al., 2004; Vanden Abeele et al., 2002; Wang et al., 2016). Both pannexin 1 and pannexin 3 have been shown to form leak channels (Ishikawa et al., 2011; Vanden Abeele et al., 2006). We identified LRRC8B as a new member of this category. Along with its localization in the ER, LRRC8B was also found in mitochondria (Fig. 6B). It would be fascinating to probe whether LRRC8B has any contribution to the ER–mitochondrial Ca^{2+} cross-talk, as other leak channels like presenilin-2 and Bcl-2 have been implicated in this process (Häcki et al., 2000; Zampese et al., 2011).

In conclusion, this study highlights the engagement of LRRC8B in Ca^{2+} homeostasis by virtue of its participation in the process of ER Ca^{2+} leak along with an effect on SOCE, being localized in the ER.

MATERIALS AND METHODS

Plasmids

Wild-type and GFP-tagged human LRRC8B (GenBank accession no. NM 015350) in pCMV6-XL5 and pCMV6-AC-GFP vectors, respectively, were procured from Origene Technologies (cat #SC120691, #RG205553). The plasmid encoding the ER Ca^{2+} indicator pCMV R-CEPIA1er (Addgene plasmid #58216) was originally deposited by Dr Masamitsu Iino, Department of Cellular and Molecular Pharmacology, University of Tokyo, Japan (Suzuki et al., 2014). The plasmid encoding the halide-sensitive YFP [pCDNA-YFP (H148Q/I152L)] was a gift from Alan Verkman (Department of Medicine, University of California, San Francisco, USA) (Galietta et al., 2001).

Antibodies and chemicals

Antibodies against LRRC8A (catalog # HPA016811), LRRC8B (catalog # HPA017950), and β-actin (catalog # A5441) were procured from Sigma-Aldrich. Antibodies against ERp72 (catalog # D70D12), Connexin 43 (catalog # 3512), VDAC (catalog # D73D12), PARP (catalogue # 46D11) were purchased from Cell Signaling Technology, and anti-Bcl-2 antibody (catalogue # sc-7382) was provided by Santa Cruz Biotechnology, USA. Fura-2-AM, Mag-Fura-2-AM and ER Tracker Red were obtained from Life Technologies, USA. DCPIB (cat #1540) was purchased from Tocris Bioscience, UK. 2-APB (catalog #D9754), Xestospongin c (catalog #X2628) and all other chemicals were procured from Sigma-Aldrich, USA. Dilutions at which antibodies are used are provided in Table S1.

Cell culture and transfection

HEK293 cells were obtained from National Centre for Cell Science, India. Cells were cultured in Dulbecco's modified Eagle's medium (DMEM), supplemented with heat-inactivated FBS (10%) in a CO_2 incubator. Cells were transiently transfected either with the plasmid containing LRRC8B, or LRRC8B tagged with GFP at its C-terminus (LRRC8B–GFP), by using Lipofectamine 2000 (Invitrogen). To suppress the expression of endogenous LRRC8B and LRRC8A, cells were transfected with siRNA against the coding sequences of human LRRC8B and LRRC8A, respectively (Sigma-Aldrich, catalog # EHU105351, # EHU001761) using Lipofectamine 2000 and a non-targeting scrambled siRNA was used as the control. GFP was co-expressed as a reporter for untagged LRRC8B and siRNA experiments.

mRNA expression analysis

Total RNA was isolated from HEK293 cells with Trizol reagent (Invitrogen). Post DNase treatment, 2 µg of RNA was converted into cDNA by using MMulV Taq from the RT-PCR kit (New England Biolabs). cDNA was then used for semi-quantitative and real-time PCR with LRRC8B-specific primers. β-actin-encoding mRNA was used as internal control. Real-time PCR was performed with a DyNAmo Color Flash SYBR Green qPCR kit (Thermo Scientific) and the fold change in gene expression was analyzed by the $2^{-\Delta\Delta CT}$ method (Schmittgen and Livak, 2008).

Estimation of cytosolic and ER Ca^{2+} levels

Cytosolic Ca^{2+} levels ($[Ca^{2+}]_c$) was measured with the ratiometric dye Fura-2 as described previously (Sahu and Bera, 2013). When Fura-2-loaded cells were permeabilized with ionomycin, the maximum $F_{340/380}$ (R_{max}) in 5 mM Ca^{2+} containing ECF was found to be ∼15–20 (varying among cell batches). This provides assurance that our estimation was not limited by the saturation of Fura-2. ER Ca^{2+} was imaged by two different methods: with the low-affinity Ca^{2+}-sensitive dye Mag-Fura-2 and with ER-targeted RCEPIA1er, a genetically encoded Ca^{2+} indicator protein that emits red fluorescence (Suzuki et al., 2014). HEK293 cells were incubated with 5 µM Mag-Fura-2-AM for 30 min at 37°C. Cells were briefly rinsed with a high K^+ solution (125 mM KCl, 25 mM NaCl, 0.1 mM $MgCl_2$, 10 mM HEPES, pH 7.2, adjusted with KOH) and then permeabilized by a quick application of digitonin (50 µg/ml), dissolved in intracellular buffer (high K^+ solution, augmented with 0.5 mM MgATP and 0.1 mM EGTA) (Vanden Abeele et al., 2002). Digitonin-permeabilized cells were then perfused with digitonin-free intracellular buffer followed by imaging at room temperature.

RCEPIAer was co-transfected with plasmids for LRRC8B overexpression or siRNA against LRRC8B in HEK293 cells. Cells were briefly washed in HBSS (140 mM NaCl, 5.6 mM KCl, 3.6 mM $NaHCO_3$, 1.8 mM $CaCl_2$, 1 mM $MgCl_2$, 5.6 mM glucose, 10 mM HEPES, pH 7.4) and then imaged for ER Ca^{2+} using the appropriate filter set. In some experiments, HBSS devoid of Ca^{2+} and supplemented with 5 mM EGTA (Ca^{2+}-free ECF), was used.

Confocal microscopy

HEK293 cells were grown on coverslips and transfected with the LRRC8B–GFP plasmid. At 24 h post transfection, cells were stained with 1 µM ER-Tracker Red for 20–30 min at 37°C. Cells were washed with HBSS and then fixed with 4% formaldehyde for 2 min at 37°C. After two more HBSS washes, cells on coverslips were mounted with VECTASHIELD anti-fade mounting medium with DAPI (Vector Laboratories) on a glass slide and observed. Fluorescence imaging was carried out using a confocal scanner on a Leica TCS SP8 microscope with a 63×, oil immersion objective.

Subcellular fractionation

ER, mitochondria, plasma membrane, nucleus and cytosol fractions were isolated as described previously (Holden and Horton, 2009; Huang et al., 2012). The successful enrichment of different cellular fractions was confirmed by western blotting, probing with respective antibodies against specific organelle markers (connexin 43 for the plasma membrane, VDAC for mitochondria, PARP for the nucleus, and ERp72 for the ER).

YFP-quenching assay

Hypotonicity-induced functional activation of LRRC8A was monitored through a YFP-quenching assay, the basis of which has been described previously (Galietta et al., 2001; Qiu et al., 2014; Voss et al., 2014). VRAC is known to transport halide anions, which is made use of in this assay. HEK293 cells were co-transfected with halide-sensitive mutant YFP (with H148Q and I152L mutations) along with respective siRNA against LRRC8A and LRRC8B. The decrease in YFP fluorescence in response to I^- was used as a read-out of the assay. Changes in fluorescence intensities upon treatment with 50 mM NaI in both isotonic and hypotonic solutions were compared.

Statistical analysis

Each experiment was repeated three to five times. The data were analyzed with Sigmaplot 13.0 software. Results are expressed as the mean±s.e.m. The *t*-test was performed for statistical comparison of the differences, and $P<0.05$ was considered significant.

Acknowledgements

The authors thank Drs Divya, Mausita and Gomathy for their critical comments.

Competing interests

The authors declare no competing or financial interests.

Author contributions

Conceptualization: A.G., A.K.B.; Methodology: A.G., N.K.; Validation: A.G.; Formal analysis: A.G., N.K.; Investigation: A.G., N.K.; Resources: A.K.B., A.K.; Data curation: A.G., N.K.; Writing - original draft: A.G., A.K.B.; Writing - review & editing: A.G., N.K., A.K., A.K.B.; Visualization: A.G., A.K.B.; Supervision: A.K.B.; Project administration: A.G., A.K.B.; Funding acquisition: A.K.B.

Funding

This work was supported by Board of Research in Nuclear Sciences (BRNS), Govt. of India [31(1)/14/55/2014-BRNS/1736].

Supplementary information

Supplementary information available online at
http://jcs.biologists.org/lookup/doi/10.1242/jcs.203646.supplemental

References

Abascal, F. and Zardoya, R. (2012). LRRC8 proteins share a common ancestor with pannexins, and may form hexameric channels involved in cell-cell communication. *BioEssays* **34**, 551-560.

Amer, M. S., Li, J., O'Regan, D. J., Steele, D. S., Porter, K. E., Sivaprasadarao, A. and Beech, D. J. (2009). Translocon closure to Ca^{2+} leak in proliferating vascular smooth muscle cells. *Am. J. Physiol. Heart Circ. Physiol.* **296**, H910-H916.
Bao, L., Locovei, S. and Dahl, G. (2004). Pannexin membrane channels are mechanosensitive conduits for ATP. *FEBS Lett.* **572**, 65-68.
Bassik, M. C., Scorrano, L., Oakes, S. A., Pozzan, T. and Korsmeyer, S. J. (2004). Phosphorylation of BCL-2 regulates ER Ca^{2+} homeostasis and apoptosis. *EMBO J.* **23**, 1207-1216.
Berridge, M. J., Bootman, M. D. and Roderick, H. L. (2003). Calcium signalling: dynamics, homeostasis and remodelling. *Nat. Rev. Mol. Cell Biol.* **4**, 517-529.
Brunello, L., Zampese, E., Florean, C., Pozzan, T., Pizzo, P. and Fasolato, C. (2009). Presenilin-2 dampens intracellular Ca^{2+} stores by increasing Ca^{2+} leakage and reducing Ca^{2+} uptake. *J. Cell. Mol. Med.* **13**, 3358-3369.
Camello, C., Lomax, R., Petersen, O. H. and Tepikin, A. V. (2002). Calcium leak from intracellular stores–the enigma of calcium signalling. *Cell Calcium* **32**, 355-361.
Choi, H., Ettinger, N., Rohrbough, J., Dikalova, A., Nguyen, H. N. and Lamb, F. S. (2016). LRRC8A channels support TNFalpha-induced superoxide production by Nox1 which is required for receptor endocytosis. *Free Radic. Biol. Med.* **101**, 413-423.
Clapham, D. E. (2007). Calcium signaling. *Cell* **131**, 1047-1058.
Fierro, L. and Parekh, A. B. (2000). Substantial depletion of the intracellular Ca^{2+} stores is required for macroscopic activation of the Ca^{2+} release-activated Ca^{2+} current in rat basophilic leukaemia cells. *J. Physiol.* **522**, 247-257.
Gaitán-Peñas, H., Gradogna, A., Laparra-Cuervo, L., Solsona, C., Fernández-Dueñas, V., Barrallo-Gimeno, A., Ciruela, F., Lakadamyali, M., Pusch, M. and Estévez, R. (2016). Investigation of LRRC8-mediated volume-regulated anion currents in *Xenopus* oocytes. *Biophy. J.* **111**, 1429-1443.
Galietta, L. J. V., Haggie, P. M. and Verkman, A. S. (2001). Green fluorescent protein-based halide indicators with improved chloride and iodide affinities. *FEBS Lett.* **499**, 220-224.
Gradogna, A., Gaitan-Penas, H., Boccaccio, A., Estevez, R. and Pusch, M. (2017). Cisplatin activates volume sensitive LRRC8 channel mediated currents in *Xenopus* oocytes. *Channels* **11**, 254-260.
Häcki, J., Egger, L., Monney, L., Conus, S., Rossé, T., Fellay, I. and Borner, C. (2000). Apoptotic crosstalk between the endoplasmic reticulum and mitochondria controlled by Bcl-2. *Oncogene* **19**, 2286-2295.
Hammadi, M., Oulidi, A., Gackiere, F., Katsogiannou, M., Slomianny, C., Roudbaraki, M., Dewailly, E., Delcourt, P., Lepage, G., Lotteau, S. et al. (2013). Modulation of ER stress and apoptosis by endoplasmic reticulum calcium leak via translocon during unfolded protein response: involvement of GRP78. *FASEB J.* **27**, 1600-1609.
Hofer, A. M., Fasolato, C. and Pozzan, T. (1998). Capacitative Ca^{2+} entry is closely linked to the filling state of internal Ca^{2+} stores: a study using simultaneous measurements of ICRAC and intraluminal [Ca^{2+}]. *J. Cell Biol.* **140**, 325-334.
Hoffmann, E. K., Lambert, I. H. and Pedersen, S. F. (2009). Physiology of cell volume regulation in vertebrates. *Physiol. Rev.* **89**, 193-277.
Holden, P. and Horton, W. A. (2009). Crude subcellular fractionation of cultured mammalian cell lines. *BMC Res. Notes* **2**, 243.
Huang, Z., Cheng, Y., Chiu, P. M., Cheung, F. M. F., Nicholls, J. M., Kwong, D. L.-W., Lee, A. W. M., Zabarovsky, E. R., Stanbridge, E. J., Lung, H. L. et al. (2012). Tumor suppressor Alpha B-crystallin (CRYAB) associates with the cadherin/catenin adherens junction and impairs NPC progression-associated properties. *Oncogene* **31**, 3709-3720.
Hyzinski-García, M. C., Rudkouskaya, A. and Mongin, A. A. (2014). LRRC8A protein is indispensable for swelling-activated and ATP-induced release of excitatory amino acids in rat astrocytes. *J. Physiol.* **592**, 4855-4862.
Ishikawa, M., Iwamoto, T., Nakamura, T., Doyle, A., Fukumoto, S. and Yamada, Y. (2011). Pannexin 3 functions as an ER Ca^{2+} channel, hemichannel, and gap junction to promote osteoblast differentiation. *J. Cell Biol.* **193**, 1257-1274.
Jentsch, T. J., Lutter, D., Planells-Cases, R., Ullrich, F. and Voss, F. K. (2016). VRAC: molecular identification as LRRC8 heteromers with differential functions. *Pflug. Archiv. Eur. J.* **468**, 385-393.
Kubota, K., Kim, J. Y., Sawada, A., Tokimasa, S., Fujisaki, H., Matsuda-Hashii, Y., Ozono, K. and Hara, J. (2004). LRRC8 involved in B cell development belongs to a novel family of leucine-rich repeat proteins. *FEBS Lett.* **564**, 147-152.
Kumar, L., Chou, J., Yee, C. S. K., Borzutzky, A., Vollmann, E. H., von Andrian, U. H., Park, S.-Y., Hollander, G., Manis, J. P., Poliani, P. L. et al. (2014). Leucine-rich repeat containing 8A (LRRC8A) is essential for T lymphocyte development and function. *J. Exp. Med.* **211**, 929-942.
Lee, C. C., Freinkman, E., Sabatini, D. M. and Ploegh, H. L. (2014). The protein synthesis inhibitor blasticidin s enters mammalian cells via leucine-rich repeat-containing protein 8D. *J. Biol. Chem.* **289**, 17124-17131.
Lutter, D., Ullrich, F., Lueck, J. C., Kempa, S. and Jentsch, T. J. (2017). Selective transport of neurotransmitters and modulators by distinct volume-regulated LRRC8 anion channels. *J. Cell Sci.* **130**, 1122-1133.
Ma, H.-T., Venkatachalam, K., Parys, J. B. and Gill, D. L. (2002). Modification of store-operated channel coupling and inositol trisphosphate receptor function by 2-aminoethoxydiphenyl borate in DT40 lymphocytes. *J. Biol. Chem.* **277**, 6915-6922.
Okada, Y. (1997). Volume expansion-sensing outward-rectifier Cl^- channel: fresh start to the molecular identity and volume sensor. *Am. J. Physiol.* **273**, C755-C789.
Pinton, P., Ferrari, D., Magalhaes, P., Schulze-Osthoff, K., Di Virgilio, F., Pozzan, T. and Rizzuto, R. (2000). Reduced loading of intracellular Ca^{2+} stores and downregulation of capacitative Ca^{2+} influx in Bcl-2-overexpressing cells. *J. Cell Biol.* **148**, 857-862.
Planells-Cases, R., Lutter, D., Guyader, C., Gerhards, N. M., Ullrich, F., Elger, D. A., Kucukosmanoglu, A., Xu, G., Voss, F. K., Reincke, S. M. et al. (2015). Subunit composition of VRAC channels determines substrate specificity and cellular resistance to Pt-based anti-cancer drugs. *EMBO J.* **34**, 2993-3008.
Qiu, Z., Dubin, A. E., Mathur, J., Tu, B., Reddy, K., Miraglia, L. J., Reinhardt, J., Orth, A. P. and Patapoutian, A. (2014). SWELL1, a plasma membrane protein, is an essential component of volume-regulated anion channel. *Cell* **157**, 447-458.
Sahu, G. and Bera, A. K. (2013). Contribution of intracellular calcium and pH in ischemic uncoupling of cardiac gap junction channels formed of connexins 43, 40, and 45: a critical function of C-terminal domain. *PLoS ONE* **8**, e60506.
Sammels, E., Parys, J. B., Missiaen, L., De Smedt, H. and Bultynck, G. (2010). Intracellular Ca^{2+} storage in health and disease: a dynamic equilibrium. *Cell Calcium* **47**, 297-314.
Sawada, A., Takihara, Y., Kim, J. Y., Matsuda-Hashii, Y., Tokimasa, S., Fujisaki, H., Kubota, K., Endo, H., Onodera, T., Ohta, H. et al. (2003). A congenital mutation of the novel gene LRRC8 causes agammaglobulinemia in humans. *J. Clin. Invest.* **112**, 1707-1713.
Schmittgen, T. D. and Livak, K. J. (2008). Analyzing real-time PCR data by the comparative C(T) method. *Nat. Protoc.* **3**, 1101-1108.
Strange, K., Emma, F. and Jackson, P. S. (1996). Cellular and molecular physiology of volume-sensitive anion channels. *Am. J. Physiol.* **270**, C711-C730.
Suzuki, J., Kanemaru, K., Ishii, K., Ohkura, M., Okubo, Y. and Iino, M. (2014). Imaging intraorganellar Ca^{2+} at subcellular resolution using CEPIA. *Nat. Commun.* **5**, 4153.
Syeda, R., Qiu, Z., Dubin, A. E., Murthy, S. E., Florendo, M. N., Mason, D. E., Mathur, J., Cahalan, S. M., Peters, E. C., Montal, M. et al. (2016). LRRC8 proteins form volume-regulated anion channels that sense ionic strength. *Cell* **164**, 499-511.
Tominaga, K., Kondo, C., Kagata, T., Hishida, T., Nishizuka, M. and Imagawa, M. (2004). The novel gene fad158, having a transmembrane domain and leucine-rich repeat, stimulates adipocyte differentiation. *J. Biol. Chem.* **279**, 34840-34848.
Tu, H., Nelson, O., Bezprozvanny, A., Wang, Z., Lee, S.-F., Hao, Y.-H., Serneels, L., De Strooper, B., Yu, G. and Bezprozvanny, I. (2006). Presenilins form ER Ca^{2+} leak channels, a function disrupted by familial Alzheimer's disease-linked mutations. *Cell* **126**, 981-993.
Ullrich, F., Reincke, S. M., Voss, F. K., Stauber, T. and Jentsch, T. J. (2016). Inactivation and anion selectivity of volume-regulated anion channels (VRACs) depend on c-terminal residues of the first extracellular loop. *J. Biol. Chem.* **291**, 17040-17048.
Van Coppenolle, F., Vanden Abeele, F., Slomianny, C., Flourakis, M., Hesketh, J., Dewailly, E. and Prevarskaya, N. (2004). Ribosome-translocon complex mediates calcium leakage from endoplasmic reticulum stores. *J. Cell Sci.* **117**, 4135-4142.
Vanden Abeele, F., Skryma, R., Shuba, Y., Van Coppenolle, F., Slomianny, C., Roudbaraki, M., Mauroy, B., Wuytack, F. and Prevarskaya, N. (2002). Bcl-2-dependent modulation of Ca^{2+} homeostasis and store-operated channels in prostate cancer cells. *Cancer Cell* **1**, 169-179.
Vanden Abeele, F., Bidaux, G., Gordienko, D., Beck, B., Panchin, Y. V., Baranova, A. V., Ivanov, D. V., Skryma, R. and Prevarskaya, N. (2006). Functional implications of calcium permeability of the channel formed by pannexin 1. *J. Cell Biol.* **174**, 535-546.
Voss, F. K., Ullrich, F., Munch, J., Lazarow, K., Lutter, D., Mah, N., Andrade-Navarro, M. A., von Kries, J. P., Stauber, T. and Jentsch, T. J. (2014). Identification of LRRC8 heteromers as an essential component of the volume-regulated anion channel VRAC. *Science* **344**, 634-638.
Wang, Q.-C., Zheng, Q., Tan, H., Zhang, B., Li, X., Yang, Y., Yu, J., Liu, Y., Chai, H., Wang, X. et al. (2016). TMCO1 Is an ER Ca^{2+} Load-Activated Ca^{2+} Channel. *Cell* **165**, 1454-1466.
Wehner, F., Olsen, H., Tinel, H., Kinne-Saffran, E. and Kinne, R. K. H. (2003). Cell volume regulation: osmolytes, osmolyte transport, and signal transduction. *Rev. Physiol. Biochem. Pharmacol.* **148**, 1-80.
Xu, C., Bailly-Maitre, B. and Reed, J. C. (2005). Endoplasmic reticulum stress: cell life and death decisions. *J. Clin. Invest.* **115**, 2656-2664.
Yamada, T., Wondergem, R., Morrison, R., Yin, V. P. and Strange, K. (2016). Leucine-rich repeat containing protein LRRC8A is essential for swelling-activated Cl^- currents and embryonic development in zebrafish. *Physiol. Rep.* **4**, e12940.
Zampese, E., Fasolato, C., Kipanyula, M. J., Bortolozzi, M., Pozzan, T. and Pizzo, P. (2011). Presenilin 2 modulates endoplasmic reticulum (ER)-mitochondria interactions and Ca^{2+} cross-talk. *Proc. Natl. Acad. Sci. USA* **108**, 2777-2782.

Supplementary figures

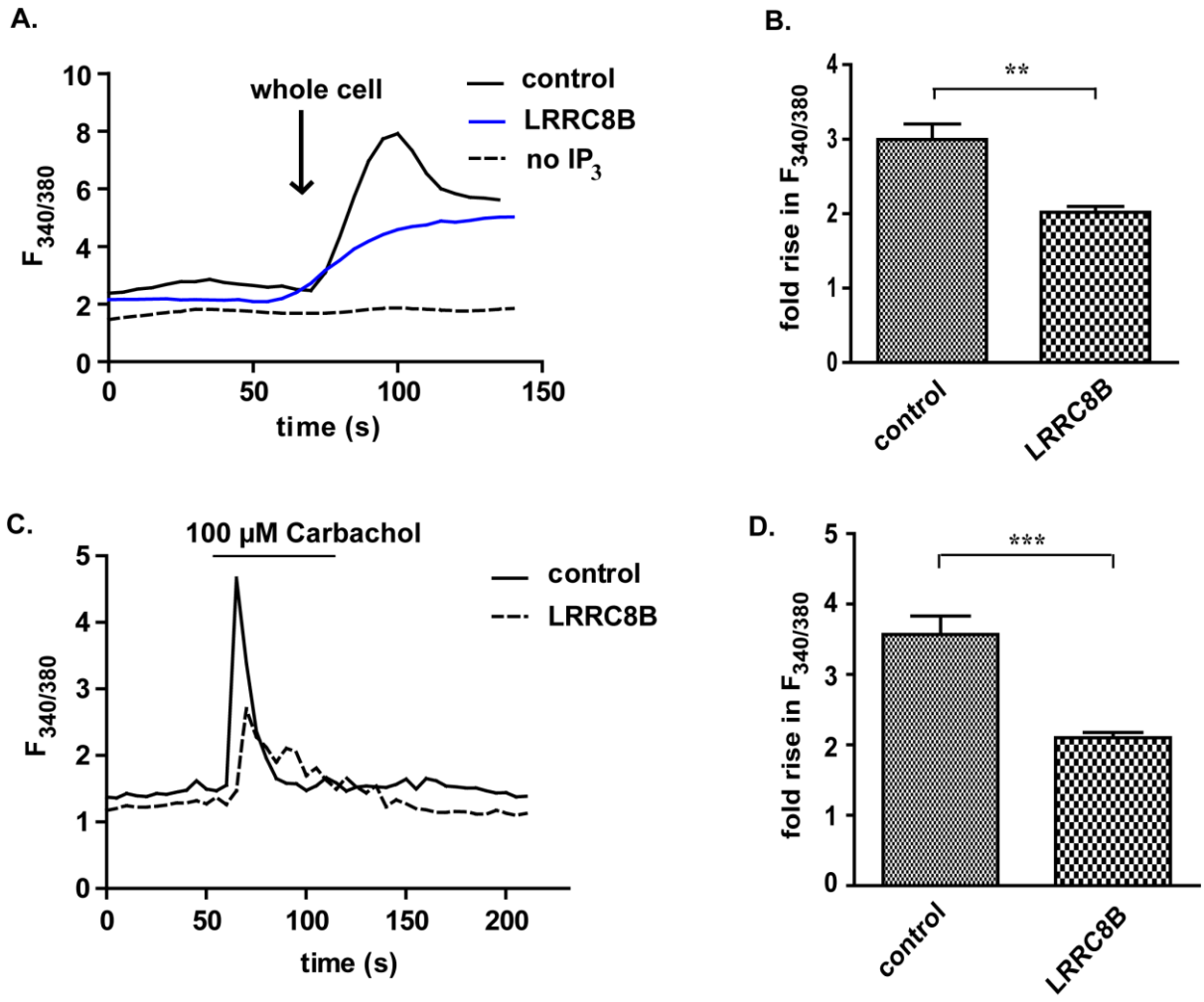

S1. Overexpression of LRRC8B supresses IP3R-activated intracellular Ca^{2+} ($[Ca^{2+}]_c$) rise

A: $[Ca^{2+}]_c$ transients evoked by injecting IP_3 (50µM) in HEK293 cells. IP_3 was administered through a patch pipette by making 'whole cell'. Both pipette solution and ECF had no Ca^{2+}. *B:* Cumulative data (mean ± SEM, n = 7-10) showing significantly lesser IP_3-induced $[Ca^{2+}]_c$ rise in LRRC8B overexpressed cells . *C:* Representative traces showing $[Ca^{2+}]_c$ rise, elicited by the application of 100 µM carbachol, in nominally Ca^{2+}-free external buffer. *D:* Cumulative data (mean ± SEM, n = 36-42) showing significantly lesser rise of $[Ca^{2+}]_c$ by carbachol in LRRC8B overexpressed cells .

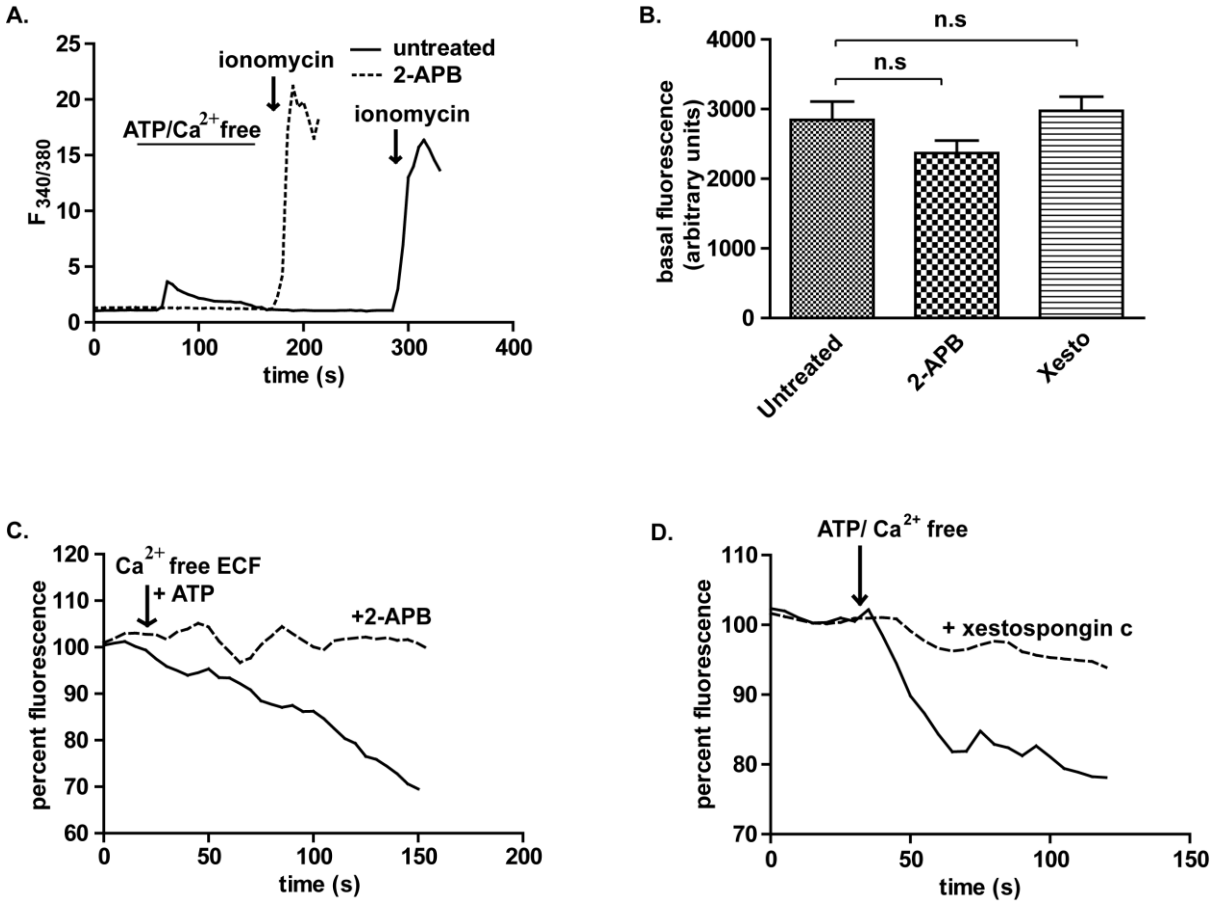

S 2. 2-APB and xestospongin c do not alter ER-Ca^{2+} stores

A: ER-Ca^{2+}stores were accessed with high concentration (5µM) of ionomycin in Ca^{2+}-free ECF. Robust rise of $[Ca^{2+}]_c$ following ionomycin treatment reflects the amount of Ca^{2+} present in stores. Both control and 2-APB treated cells exhibited ionomycin-mediated $[Ca^{2+}]_c$ rise to the similar extent. Cells were first incubated with or without 2-APB for 10 mins, after which ATP was applied in Ca^{2+}-free ECF. Then ionomycin (in Ca^{2+}-free ECF) was applied to release ER-Ca^{2+}. ATP (100µM) caused a rise in $[Ca^{2+}]_c$ in control cells but not in 2-APB

treated cells. *B:* ER-Ca^{2+} imaging with ER-targeted Ca^{2+} indicator RCEPIA1er reveals no significant difference in basal $[Ca^{2+}]_{ER}$ between untreated HEK293 cells and cells subjected to 2-APB (50µM) and xestospongin c (5µM) treatment. *C:*and *D:* Ca^{2+} imaging in ER reveals no notable decay of luminal Ca^{2+} following ATP treatment (in Ca^{+2}-free ECF) in 2-APB (50µM) and xestospongin c (3 µM)-treated cells. Untreated control cells (no blocker) showed quick release of ($[Ca^{2+}]_{ER}$ by ATP.

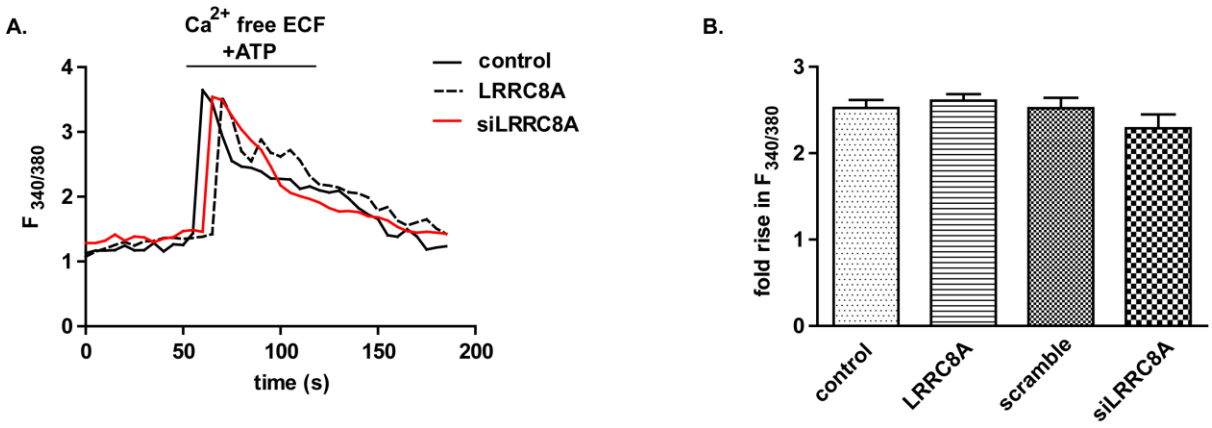

S 3. LRRC8A does not affect ATP-induced release of Ca^{2+} from stores.

A: Characteristic $[Ca^{2+}]_c$ traces in response to 100 µM ATP in nominally Ca^{2+}-free external buffer in HEK-293 Cells. Overexpression or knockdown of LRRC8A did not affect ATP-induced $[Ca^{2+}]_c$ rise. *B:* Cumulative data (mean ± SEM, n = 41-50) showing the level of LRRC8A does not influence $[Ca^{2+}]_c$ rise elicited by ATP in Ca^{2+}-free conditions.

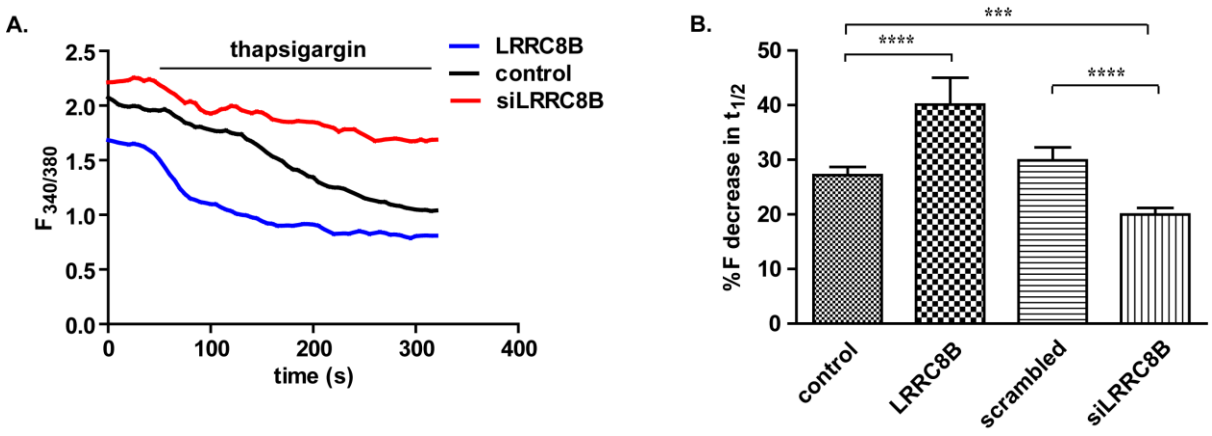

S 4. Modulation of $[Ca^{2+}]_{ER}$ leak rate by LRRC8B.

A: Typical traces showing the decay of luminal Ca^{2+} ($[Ca^{2+}]_{ER}$), by blocking SERCA pump with 1µM TG. $[Ca^{2+}]_{ER}$ was measured with Mag-fura, as described in methods section. LRRC8B overexpressed and knocked down increased and decreased the decay rate respectively. *B:* Cumulative data for decrease in % fluorescence in $t_{1/2}$ (mean ± SEM, n = 16-27) are plotted.

Table S1. Antibody Validation

Protein	Antibody catalogue no.	Company	References	Dilution
LRRC8A	# HPA016811	Sigma Aldrich	Voss FK et. al Science, 344(6184), 634-638 (2014)	1:500
LRRC8B	# HPA017950	Sigma Aldrich	Voss FK et. al Science, 344(6184), 634-638 (2014)	1:500
β-actin	# A5441	Sigma Aldrich	Hu W et. al PNAS, 107(16), 7455-7460 (2010)	1:1000
ERp72	# D70D12	Cell SignallingTechnology	Kebede MA et al. *J Clin Invest.* 2014 Oct;124(10):4240-56	1:1000
Connexin 43	#3512	Cell Signalling Technology	Nimlamool W et al. *Mol Biol Cell.* 2015 Aug1;26(15):2755-	1:1000

			68.	
VDAC	# D73D12	Cell Signalling Technology	Tewari D et al. Biochim Biophys Acta 1848 (1 Pt A), 151-158. 2014 Oct 23	1:1000
PARP	# 46D11	Cell Signalling Technology	De Waal L et al. *Nat Chem Biol.* 2016 Feb;12(2):102-8.	1:1000
Bcl2	# sc-7382	Santa Cruz Biotechnology	Pilchova I et al. *Cell Mol Neurobiol.* 2015 Jan;35(1):23-31	1:750